

UNIVERSITY OF OKLAHOMA

GRADUATE COLLEGE

COMMUNITY VULNERABILITY PERSPECTIVES ON INFRASTRUCTURE

NETWORK RESILIENCE DECISION MAKING

A THESIS

SUBMITTED TO THE GRADUATE FACULTY

in partial fulfillment of the requirements for the

Degree of

MASTER OF SCIENCE

By

DENIZ BERFIN KARAKOC

Norman, Oklahoma

2019

COMMUNITY VULNERABILITY PERSPECTIVES ON INFRASTRUCTURE
NETWORK RESILIENCE DECISION MAKING

A THESIS APPROVED FOR THE
SCHOOL OF INDUSTRIAL AND SYSTEMS ENGINEERING

BY

Dr. Kash Barker, Chair

Dr. Shima Mohebbi

Dr. Andrés González

© Copyright by DENIZ BERFIN KARAKOC 2019

All Rights Reserved.

Acknowledgments

I would like to express my sincere gratitude to my advisor Dr. Kash Barker, who has supported me through my entire research study. He has consistently encouraged me to produce my own work and express my original ideas. He has always steered me in the right direction with his infinite wisdom whenever I came across a challenge.

I would also like to thank Dr. Shima Mohebbi and Dr. Andrés González for being a part of my thesis committee who enriched my work with their essential reviews, time and efforts.

Additionally, I would like to thank my family, my parents Guleser and Ali Karakoc, and my sister Damla Karakoc for supporting me spiritually throughout my degree and life. Their love and guidance always give me the strength I needed.

Last but not least, I would like to offer my appreciation especially to my beloved significant other Muslum Ozgur Ozmen. Most importantly, his continuous support, unlimited love, and unfailing patience were the fundamental encouragement for me through this experience. I wouldn't be where I am without him as he was always there for me to set higher goals and accomplish them.

Table of Contents

Acknowledgments.....	iv
Table of Contents	v
List of Tables	vii
List of Figures.....	viii
Abstract	xi
Chapter 1: Introduction and Motivation	1
Chapter 2: Methodological Background.....	9
2.1 Modeling and Measuring Network Resilience.....	9
2.2 Restoring Interdependent Infrastructure Networks	11
2.3 Characterizing Social Vulnerability	13
2.4. Social Equity Aspect	16
Chapter 3: Proposed Methodology	18
3.1. Interdependent Infrastructure Network Restoration Model	18
3.1.1. Notation and Assumptions	18
3.1.2. Community Resilience Measures	20
3.1.3. Optimization Model	22
3.2. Resilience-Driven Component Importance Measure	26
3.2.1. Notation and Assumptions.....	26

3.2.2. Social Vulnerability Measures	27
3.2.3. Optimization Model	27
3.2.4. Component Importance Measure	29
3.2.5. Multi-criteria Decision Analysis Technique for Aggregated Ranking	30
Chapter 4: Illustrative Example	32
4.1. Interdependent Infrastructure Network Restoration.....	32
4.1.1. Social Vulnerability in Shelby County, TN	33
4.1.2. Disruption and Restoration	42
4.2. Resilience-Driven Component Importance Measure	50
4.2.1. Social Vulnerability Variables	51
4.2.3. Disruption Scenarios	54
4.2.4. Integration of Rankings with TOPSIS	55
4.2.5. Critical Components of Shelby County, TN.....	58
Chapter 5: Concluding Remarks	61
References	65

List of Tables

Table 1. The 11 factor groups that are identified by Cutter et al. [2003] to quantify the social vulnerability of a community.....	15
Table 2. Percentage based district-level social vulnerability variables available in Shelby County, TN data for the SoVI-Lite algorithm.	33
Table 3. The percentage based social vulnerability variables that are utilized through the SoVI-Lite algorithm for the block group level in Shelby County, TN.....	38
Table 4. The complete final list of the social vulnerability variables that are utilized in the community-resilience study of Shelby County, TN which are defined by Cutter et al. [2003] as the percentages.....	52
Table 5. The representation of the weights of the social vulnerability variables that are determined by PCA method and utilized in TOPSIS algorithm.	57
Table 6. A subset of the critical components (both nodes and links are considered) in the water and power network based on all the available social vulnerability measures together.	60

List of Figures

Figure 1. Relationship between physical infrastructure and community networks (adapted from Barker et al. [2017]).	4
Figure 2. Network performance representation, $\varphi(t)$, across various stages of a disruptive event (adapted from Henry and Ramirez-Marquez et al. [2012]).	10
Figure 3. Critical (a) water, (b) gas, and (c) power infrastructure networks of Shelby County, TN and (d) their physical interdependencies respectively (adapted from González et al. [2016]).	33
Figure 4. An illustration of the correlation analysis between the 14 social vulnerability variables available for the district level in Shelby County, TN, where darker red color and bigger circle size represent a higher negative correlation and darker blue color and bigger circle size represent a higher positive correlation.	35
Figure 5. An illustration of the correlation analysis with the available social vulnerability variables in the block group level in Shelby County, TN, where darker red color and bigger circle size represent a higher negative correlation and darker blue color and bigger circle size represent a higher positive correlation.	37
Figure 6. An illustration of the distribution of block groups into Voronoi cells that are created by the demand nodes of three critical infrastructure networks in Shelby County, TN.	39
Figure 7. Illustration of social vulnerability indices, $SoVI_{ik}$ of the demand nodes.	40
Figure 8. Illustration of the exponential social vulnerability scores, V_{ik} .	41
Figure 9. Representation of the exponential social vulnerability scores, V_{ik} , of the demand nodes of all three critical infrastructure networks over Shelby County, TN.	41
Figure 10. The change in the importance of the disrupted supply, transshipment, and demand nodes in the water network when the community perspective is considered with the earthquake	

magnitude $M_w = 8$, where lighter blue represents higher negative change and darker blue represents higher positive change.	44
Figure 11. The change in the importance of the disrupted supply, transshipment, and demand nodes in the gas network when the community perspective is considered with the earthquake magnitude $M_w = 8$, where lighter green represents higher negative change and darker green represents higher positive change.	44
Figure 12. The change in the importance of the disrupted supply, transshipment, and demand nodes in the power network when the community perspective is considered with the earthquake magnitude $M_w = 8$, where lighter orange represents higher negative change and darker orange represents higher positive change.	45
Figure 13. The change in the importance of the disrupted supply, transshipment, and demand nodes in the water network when the community perspective is considered with the earthquake magnitude $M_w = 9$, where lighter blue represents higher negative change and darker blue represents higher positive change.	46
Figure 14. The change in the importance of the disrupted supply, transshipment, and demand nodes in the gas network when the community perspective is considered with the earthquake magnitude $M_w = 9$, where lighter green represents higher negative change and darker green represents higher positive change.	47
Figure 15. The change in the importance of the disrupted supply, transshipment, and demand nodes in the power network when the community perspective is considered with the earthquake magnitude $M_w = 9$, where lighter orange represents higher negative change and darker orange represents higher positive change.	48

Figure 16. Illustration of unmet demand over the recovery time (a) without SoVI, (b) with SoVI, and (c) comparison on the same plot where dashed lines represent the consideration and solid lines represent the inconsideration of social vulnerability and population density. 49

Figure 17. The geographic layout of power and water distribution systems in Shelby County, TN independently and interdependently, respectively (adapted from González et al. [2016]). 51

Figure 18. The distribution of social vulnerability scores over the block groups in Shelby County, TN based on the population that is (a) under age five, (b) over age sixty-five, (c) Hispanic, (d) living in poverty, and (e) living in a single-female household whereas with the darker shades, socially more vulnerable region is represented..... 53

Figure 20. The ranking of the subset of power network components (both nodes and links are listed) are represented independently based on each social vulnerability variable. 59

Figure 19. The ranking of the subset of the water network components (both nodes and links are listed) are represented independently based on each social vulnerability variable. 59

Abstract

Critical interdependent infrastructure networks such as water distribution, natural gas pipeline, electricity power, communication and transportation systems provide the essential necessities for societies and their utilization is the backbone of everyday processes such as production, health, convenience and many more. Often cascading dysfunctionality or disruption in these critical infrastructure networks triggers chain reactions of blackouts or blockages through the system of highly interconnected infrastructure networks and the inevitable collapse of surrounding societies. For the planning of restoration processes and resilience of these, social aspects and demographics should also be considered to assign and mitigate the possible social risks associated with these disruptions. Additionally, it is crucial to identify the most critical components of these networks which are the components that have the largest impact on the performance of both their and other networks that are operationally dependent. These critical components have the largest impact on society in terms of serving its needs so that its recovery can be completed in a timely manner after a disruption. This research studies the restoration planning of critical interdependent infrastructure networks after a possible disruptive event by mainly emphasizing on the vulnerability indices of interacting society. The methodology integrates (i) a resilience-driven multi-objective mixed-integer programming formulation to schedule the restoration process of disrupted network components in each network, and (ii) a component importance measure that quantifies the impact of equitable restoration activities on components with (iii) an index of social vulnerability that is geographically distributed. An illustrative example of the proposed integrated model that focuses on studying the community resilience in Shelby County, TN, United States is also represented.

Chapter 1: Introduction and Motivation

Modern societies heavily rely on the sustainability and proper performance of critical infrastructure networks. Two decades ago, the Report of the President's Commission on Critical Infrastructure Protection [1997] defined a critical infrastructure network as a "network of independent, mostly privately-owned, man-made systems and processes that function collaboratively and synergistically to produce and distribute a continuous flow of essential goods and services. These critical infrastructure networks such as water distribution, electric power, natural gas, communication, and transportation systems are essential for providing the basic human needs of the societies and maintaining their quality of life. However, more recently Infrastructure Security Partnership [2011] emphasized the importance of forming physically interdependent infrastructure networks that are resilient against the disruptions that will eventually occur. They defined resilient infrastructure networks as the networks that should "prepare for, prevent, protect against, respond or mitigate any anticipated or unexpected significant threat or event" and that are able to "rapidly recover and reconstitute critical assets, operations, and services with minimum damage and disruption". Additionally, the National Infrastructure Protection Plan [DHS 2013] focuses on the enhancement of risk and vulnerability due to the interdependencies among the infrastructure networks and the importance of addressing these issues through the planning and forming of infrastructure by stating that it is "essential to enhancing critical infrastructure security and resilience" against inevitable disruptions, perhaps with more frequency, due to natural disasters, malevolent attacks, and aging-driven failures. Hence, as it has been highlighted by the White House [2013], the planning phase of infrastructure networks is more targeted to maintain "secure, functioning, and resilient critical infrastructures".

While measuring the vulnerability of infrastructure networks by either topological descriptors [Barabasi and Albert 1999, Holmgren 2006, Newman et al. 2006, Nagurney and Qiang 2009] or by flow-based descriptors [Rocco et al. 2010, Ouyang 2014, LaRocca et al. 2014, Nicholson et al. 2016] has been a well-studied problem, the restoration of infrastructure networks has been an important area of study for the last decade, particularly from an optimization perspective. The stochastic integer program proposed by Xu et al. [2007] determines the schedule of inspection, damage assessment, and repair tasks that optimize the power network restoration. Yan and Shih [2009] proposed a multi-objective, mixed-integer programming method with the objective of minimizing the total time of repair and relief distribution after a disruption in a transportation network. Similarly, Matisziw et al. [2010] developed a multi-objective optimization model to maximize the total system flow while minimizing the system cost through the recovery of a communication system. The integer programming model by Nurre et al. [2012] considers the maximization of the cumulative weighted flow in the infrastructure networks by scheduling work crews to restore disrupted components. Aksu and Ozdamar [2014] proposed a dynamic path based mathematical model to maximize network accessibility by scheduling debris removal. Vugrin et al. [2014] developed a bi-level optimization model for network recovery, providing the recovery sequence that maximizes the total flow in a critical infrastructure network. The multi-objective optimization model developed by Kamamura et al. [2015] focuses on the recovery of transportation systems by maximizing the traffic recovery ratio and minimizing the number of switched transportation paths in each stage of a multi-stage restoration process. Finally, Fang et al. [2016] proposed a Monte Carlo simulation-based method to rank the disrupted components according to their impact on system resilience to order their recovery. In general, the previously proposed algorithms commonly cover the objective of maximizing the performance of

infrastructure networks, rebuilding the disrupted components and their overall functionality by assigning the disrupted components to work crews, and determining the order of restoration sequence in the aftermath of a disruption. However, we believe that integrating the existing infrastructure restoration studies with a social perspective could be important for communities considering societal needs and focusing on the social benefits of infrastructure restoration. Hence, in this study, we model the restoration scheduling of critical interdependent infrastructure networks from a community resilience perspective.

As noted by Rinaldi et al. [2001], infrastructure networks do not exist and function on their own in an isolated environment. In fact, they often rely heavily on each other in various ways. The interdependency of infrastructure networks has been categorized into four groups [Rinaldi et al. 2001]: (i) physical, where output from one infrastructure network serves as an input to another, (ii) cyber, where one network depends on the information transmitted from another, (iii) geographical, where two infrastructure networks can be affected by the same local disruptive event, and (iv) logical, for all other possible types of dependency. Figure 1 represents the interdependencies between different main infrastructure networks that exist in a modern-day society. In this study, we only focus on the physical interdependency between three major infrastructure networks, though the proposed approach is generalizable for considering other types of interdependencies as well.

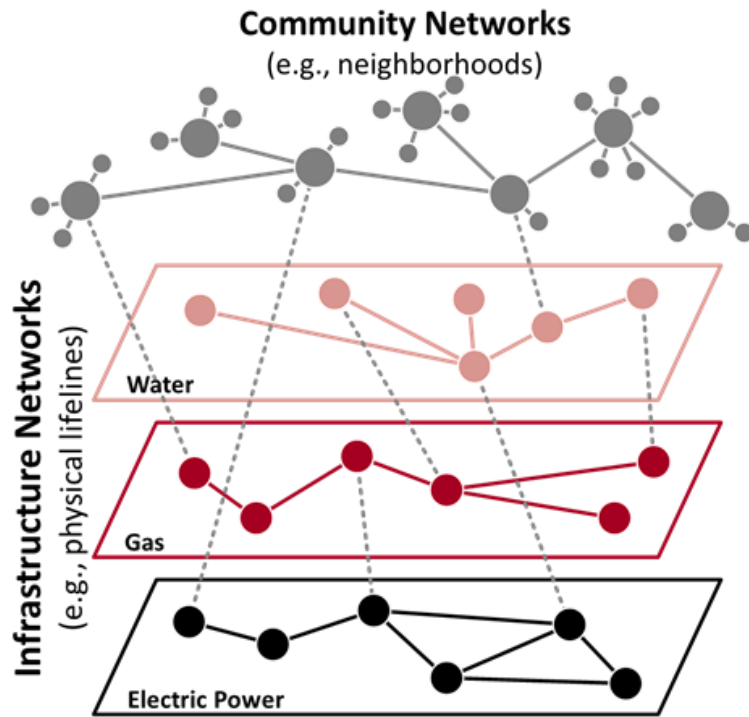


Figure 1. Relationship between physical infrastructure and community networks (adapted from Barker et al. [2017]).

Interdependencies among infrastructure networks become more frequent and complex due to the increasing trend of globalization and technological developments [Castells 1996, Graham 2000, Graham 2000, Rinaldi et al. 2001]. Even though the interdependencies can improve the efficiency of network functionality, this type of complex coordination causes them to become more vulnerable to disruptions. As a result of the interdependency, a disruption in some components of one of the infrastructure networks could lead a dysfunctionality in the undisrupted components of other dependent networks and could result in a series of cascading failures among the whole infrastructure network system [Little 2002, Wallace et al. 2003, Buldyrev et al. 2010, Eusgeld et al. 2011]. Therefore, this high vulnerability of infrastructure networks against disruptions is a critical concern for decision makers where they should account for the interdependencies through the recovery planning to achieve a realistic performance analysis [Holden et al. 2013]. Moreover, scheduling the restoration processes separately for interdependent infrastructure networks without

considering their interdependencies could cause misutilization of resources, waste of time and funds, and even might trigger additional inoperability of distribution systems [Baidya and Sun 2017]. However, functional connectivity among these critical infrastructures is not the only dependency that should be taken into account. The supply-demand relationship, thus an existence-based dependency that exists within cyber-physical-social systems, is another challenging aspect that should be addressed in restoration scheduling models.

As infrastructure networks exist to enable the fundamental services that support the economic productivity, security, and quality of life of the community, interdependency among infrastructures is not the sole interdependency of interest in this study. Defined as the interconnected society that infrastructure networks support [Barker et al. 2017], we are also interested in community networks. The interdependency among these infrastructure and community networks is generally depicted in Figure 1. Among the planning documents by government agencies on resilience, there is a particular emphasis on the resilience of communities after a disruptive event. The National Academies of Science [2012] suggests “One way to reduce the impacts of disasters on the nation and its communities is to invest in enhancing resilience [...].” The National Institute for Standards and Technology [2015] defines community resilience as “the ability of a community to prepare for anticipated hazards, adapt to changing conditions, and withstand and recover rapidly from disruptions.” Community resilience is the ability of a community to successfully cope with disruptions from the economic, social, and environmental aspects, as well as to coordinate recovery activities [Rotmans et al. 2003, Resilience Alliance 2009]. As such, communities contribute to the overall impact of a disruption and should be considered in modeling infrastructure restoration.

Considering the equity through the preparedness and recovery activities against disruptions is another critical humanitarian approach [Gralla et al. 2014, Huang et al. 2012]. Especially in disaster relief efforts and humanitarian supply chain management, social equity is addressed such that (i) the optimal distribution of relief goods or demanded commodities to the affected society ensures that an equitable amount of goods are provided to each portion of the community [Davis et al. 2013, Noyan et al. 2016] or (ii) the relief efforts and allocation of resources are reshaped based on the varying vulnerability, expectations, and social demographics of the different groups [Arnette and Zobel 2019, and Zolfaghari and Peyghaleh 2015].

Different components in the infrastructure networks can have different impacts on its own network, as well as other interdependent infrastructure and community networks. For example, the outage of a particular electric power substation could adversely impact the entire power grid, the water and telecommunications networks that require electricity, and several populations, some of which could be vulnerable during times of disruption. As such, it is important to identify the critical components of the infrastructure networks to understand their impacts and to effectively plan for their restoration. The identification of critical components has been aided by component importance measures (CIMs), long studied in the reliability engineering literature. Particularly for networks, topology-driven CIMs rank components by average path length [Newman 2006] and network efficiency [Nagurney and Qiang 2009], while flow-driven CIMs have been developed for various vulnerability measures [Nicholson et al. 2016, Ouyang et al. 2014, Rocco et al. 2010]. Several importance measures have been developed to capture network resilience [Barker et al. 2013, Whitson and Ramirez-Marquez 2009], including recoverability-driven CIMs identified by their optimal repair time and their role in reducing resilience [Fang et al. 2016]. Several CIMs have been developed for interdependent networks, including: (i) interdependent rank ordering, which

considers physical interdependency among and ranks each node separately for multiple importance criteria (i.e., network connectivity, flow transfer, network vulnerability, flow traversal), (ii) geographic valued worth, which ranks geographic locations by the disruption impact of that location over the multiple, geographically interdependent networks, (iii) a CIM that ranks components in interdependent networks according to their synergistic consequences over the total synergistic consequences for a specific failure set [Johansson and Hassel 2010], and (iv) a CIM that evaluates network components according to the drop in the network performance that is caused by their one-at-a-time disruption [Wang et al. 2013].

This research studies the restoration of interdependent infrastructure networks from the perspective of community impact as measured by socio-economic and demographic information describing the affected communities and develops a resilience-driven CIM that combines (i) interdependent infrastructure network restoration with (ii) impact on the community that those infrastructure network components serve. The social vulnerability indices [Cutter et al. 2003] and population densities of the service areas are used to represent community impact, thus guiding the restoration process toward areas of potential community need. The primary objective of the interdependent infrastructure networks restoration study is to: (i) integrate a resilience-driven multi-objective mixed-integer programming formulation to schedule the restoration of disrupted components in each network, (ii) assign the restoration of these components to specific work crews, and (iii) prioritize them with social vulnerability indices and densities of the covered population in order to measure the expectations of the geographically surrounding community. For identifying the critical components of the interdependent infrastructure networks, this research considers (i) several dimensions of social vulnerability, driven by the Social Vulnerability Index [Cutter et al. 2003], (ii) ranking the components separately according to those dimensions then (iii)

aggregating them using a multi-criteria decision analysis technique. This proposed approach provides a new perspective on infrastructure network component importance that ties to social equity and community resilience.

The remainder of this study is organized as follows. In Chapter 2, the methodological background that the proposed approach is built upon is explained, in Chapter 3 the proposed mixed-integer multi-objective resilience-driven optimization model for interdependent infrastructure network restoration problem and the adopted component importance measure in the study is defined and in Chapter 4 the illustrative example of the proposed study is included over the critical infrastructure networks in Shelby County, TN. Finally, Chapter 5 is followed by the concluding remarks of this research.

Chapter 2: Methodological Background

In this chapter, the relevant methodological background on network resilience measures, independent infrastructure network recovery problems, social equity aspects, and social vulnerability indices are addressed.

2.1 Modeling and Measuring Network Resilience

Resilience is often considered to be the ability to withstand, adapt to, and recover from a disruption [Obama 2013]. While many generally agree on the definition [Haines 2009, Aven 2011, Ayyub 2011], a number of approaches to measure and model resilience have been proposed in the recent literature [Hosseini et al. 2016]. For example, Cimellaro et al. [2010] measured the resilience of a system as the normalized area underneath a function describing the performance of the system, while, Rosenkrantz et al. [2009] represented resilience as a function of topological measures, and Li and Lence [2007] quantified resilience as the probability of failure recovery.

In this study, the resilience of a network is quantified by adopting the paradigm proposed by Henry and Ramirez-Marquez [2012]. Denoted as \mathcal{R} , the resilience of a network at time t is formulated as $\mathcal{R}(t|e^j) = \text{Recovery}(t)/\text{Loss}(t_d)$, for disruptive event e^j and where $t_d < t < t_f$ as shown in Figure 2.

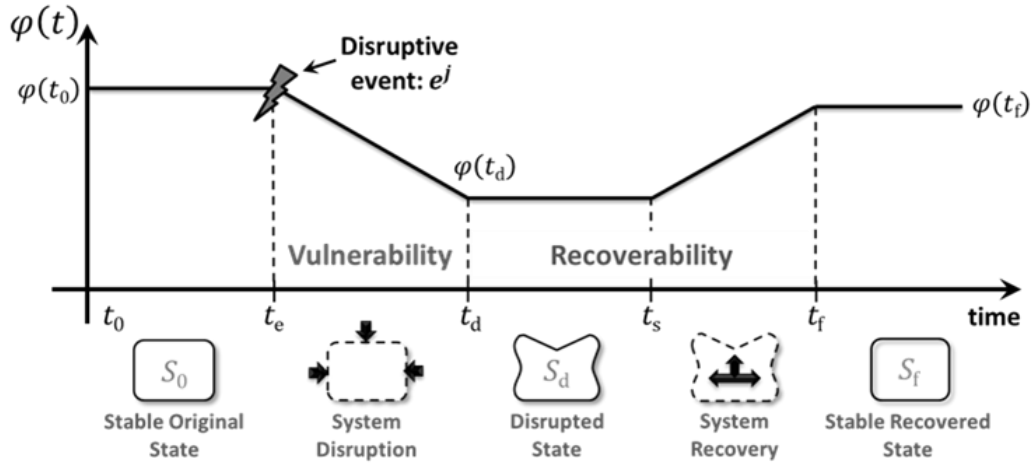


Figure 2. Network performance representation, $\varphi(t)$, across various stages of a disruptive event (adapted from Henry and Ramirez-Marquez et al. [2012]).

As it is illustrated in Figure 2, the two primary dimensions of network resilience are vulnerability and recoverability [Henry and Ramirez-Marquez 2012, Barker et al. 2013], and their definitions in the literature as follow: Jönsson et al. [2008] defined vulnerability of a network as “the magnitude of damage in network performance due to a disruptive event” and Rose [2007] referred recoverability of a network as “the speed at which the network reaches to a desired performance level”.

In a more detailed discussion, Figure 2 represents the three transition stages of the occurrence of a disruptive event in a system; before, during and after. The stage of network before the occurrence of a disruptive event, e^j , at time t_e , is the original stable state, S_0 . The disrupted stage of the network where the maximum disruption occurs from time t_e to time t_d is represented as S_d and this state continues until the restoration process begins at time t_s . Finally, the recovered state of the network is denoted with S_f and this is the state where the restoration process of the disrupted components are completed at time t_f . Additionally, the performance of the network or the system is represented by $\varphi(t)$ through the illustration which states the flow, connectivity,

unmet demand or delay through the three states. The network performance before the occurrence of a disruptive event is represented as $\varphi(t_0)$, the performance through the disruption until the completeness of restoration process is stated as $\varphi(t_d)$ which could be less than the original performance, $\varphi(t_0)$, since the system is affected by the disruption and the connectivity, flow, or the utilization of the assets could be damaged. Finally, the desired level of network performance after the completion of the restoration process is represented as $\varphi(t_f)$ where it does not have to be same with the performance at the original state $\varphi(t_0)$, it could be less or more according to the network properties.

2.2 Restoring Interdependent Infrastructure Networks

Attention has recently been devoted to studying the optimal scheduling of restoration resources for interdependent infrastructure networks. Lee et al. [2007] proposed an interdependent layered network model using mixed-integer programming with the objective of minimizing the sum of costs associated with flow and slack through the time, where cost and available work crews for restoration were not accounted for. Gong et al. [2009] proposed an optimization model for the restoration of disrupted interdependent network components assuming that the predetermined due dates of these components as the upper-limit on the completion of the restoration process are known through the study. Their multi-objective restoration scheduling model was solved using Benders decomposition with the objective of minimizing the cost, tardiness, and makespan. Coffrin et al. [2012] proposed an integrated mixed-integer programming method to maximize the weighted sum of interdependent met demand through the recovery duration. Cavdaroglu et al. [2013] and Sharkey et al. [2015] proposed mixed-integer programming models to determine the set of disrupted components that should be restored and to assign them to available work crews with the objective of minimizing the sum of flow cost, slack cost, and the cost associated with the

restoration process (e.g., installation and assignment of disrupted components). Holden et al. [2013] studied an extended network-flow model at a local-scale of physically interdependent infrastructure networks to simulate their performance by providing a linear programming optimization model that minimized the total cost of production, commodity flow, storage, discharge, and slack demand. González et al. [2016] proposed the Interdependent Network Design Problem (INDP), which focuses on finding the optimal recovery strategy of a system of interdependent networks, while considering limited resources, possible savings due simultaneous repairs of co-located components, and other budget and operational constraints. Smith et al. [2017] proposed a game-theory-based model to study and optimize the recovery of system of interdependent networks when each network is separately managed by a different entity (or player). González et al. [2017] proposed a data-driven system identification approach that uses a linear operator (defined as the recovery operator) to depict the main damage and recovery dynamics of a system of interdependent networks, which later on can be used to efficiently generate quasi-optimal recovery strategies. Baidya and Sun [2017] formulated a mixed-integer linear programming approach to prioritize the restoration activities of disrupted components in the physically interdependent power and communications infrastructure networks with the objective of minimizing the number of energizing activities required through the restoration to ensure the operability of every node. Tootaghaj et al. [2017] proposed a two-phase recovery approach for physically interdependent power and communications network while assuming that the disruption occurred only in the power network. First, the formulation of a linear programming model for minimum flow cost assignment problem to avoid further failures in the system is completed. The objective of this model is finding the setting of the power flow which avoids further cascading. Then, the formulation of a mixed-integer programming for the recovery problem of these

interdependent infrastructure networks in order to provide the schedule of recovery for the disrupted components took place. The objective of this approach is to maximize the total amount of commodity delivered through both networks (i.e. electricity power) in the recovery duration. Zhang et al. [2018] proposed an optimization model to determine the allocation of available restoration resources (i.e., time and work crews) and the optimal budget associated with the restoration process after a specific disruption scenario for the physically interdependent infrastructure networks while the resilience of the system is enhanced. In the literature, even though the restoration scheduling of interdependent infrastructure networks has been examined both with network performance and resilience perspective in mind, accounting for the resilience of communities is the most important contribution of this work.

In this research, a generic approach to account for community resilience in a multi-objective optimization model (adopted from Almoghathawi et al. [2017]) is proposed. The model considers time availability and specific skill requirements in the work crews for the restoration of disrupted components (i.e., each network has been assigned with different work crews for the restoration process). The two objectives are (i) maximizing the resilience of studied interdependent infrastructure networks, and (ii) minimizing the costs associated with the disruption, resulting unsatisfied demand, and restoration. Discussed subsequently, the model proposed in this paper accounts for the social vulnerability and population densities associated with the disrupted components of the interdependent networks.

2.3 Characterizing Social Vulnerability

In defining network vulnerability in a holistic way, Mileti [1999] focused on the impacts of the surrounding environment vulnerabilities from three perspectives: (i) the physical environment, (ii) the constructed structures, and (iii) the served society. The first perspective deals

with the spatial characteristics of the setting of an infrastructure network and could be quantified with spatially-explicit information (i.e. location of the network components) [Mileti 1999] and the evacuation potential of the study region (in arterial miles/mi²) [NRC 2006]. The second perspective deals with the vulnerability of structures, such as which could be quantified the housing age [NRC 2006] and tree trimming frequency of the region [Guikema et al. 2006]. With regard to the third perspective, on understanding the vulnerability level of the served society, more human and community characteristics are considered. For example, in terms of the restoration resources some studies utilized the number of available resources (i.e., restoration work crews and equipment, physicians and emergency responders) in the region [Norris et al. 2008], the shelter capacity of the area [Tierney 2009], and the medical capacity of the considered location [Auf der Heide and Scanlon 2007], among others. Other studies have emphasized the importance of socio-economic demographics to describe the vulnerability of the served society. For example, Norris et al. [2008] and Cutter et al. [2008] focused on racial and ethnic inequalities in communities, Norris et al. [2008] and Morrow [2002] focused on educational inequality, and Cutter et al. [2008] analyzed previous disaster experience.

Social vulnerability is defined as the set of characteristics of an individual or a group in terms of their capacity to anticipate, cope with, resist, and recover from the impact of a hazard [Blaikie et al. 1994]. Many take a socio-economic approach to model social vulnerability, as such socio-economic measures that represent the inherent vulnerabilities of certain demographic groups where due to these different natures, the consequences of the same disruption over different communities would not be same [Cutter et al. 2003, Morrow 2002, Cutter et al. 2008, Tierney 2009]. One such model is the Social Vulnerability Index (SoVI). Cutter et al. [2003] developed the SoVI algorithm to identify the socially more vulnerable groups in society and formulate a final

aggregated index describing the cumulative effect of individual socioeconomic characteristics. In the SoVI algorithm, the 42 socio-economic characteristics are defined as social vulnerability variables as each one of them represent a different sub-group in the society. Also, these variables are grouped into eleven social vulnerability factors and they are listed in Table 1.

Table 1. The 11 factor groups that are identified by Cutter et al. [2003] to quantify the social vulnerability of a community.

Age	Occupation
Density of the built environment	Personal wealth
Ethnicity (Hispanic)	Race (African-American)
Ethnicity (Native American)	Race (Asian)
Housing stock and tenancy	Single-sector economic dependence
Infrastructure dependence	

According to the definitions and percentages of these factors, these various properties either oppose or contribute to the community resilience measure of a region. By utilizing these 11 factor groups of factors, Cutter et al. [2003] then developed a social vulnerability index algorithm to calculate the vulnerability of spatially explicit communities, suggesting that the utilization of available resources through the pre- and post-disruption stages may differ for each community.

In this study, a reduced version of the SoVI algorithm, SoVI-Lite [Cutter et al. 2013, Evans et al. 2014], is utilized to measure the potential of community loss and possible community response in after a disruption. Thus, the SoVI-Lite algorithm is used here as a community resilience indicator to guide the restoration scheduling problem for disrupted interdependent infrastructure networks.

The SoVI-Lite algorithm calculates the social vulnerability index for a given community with the following three steps: (i) obtaining the percentage of the population in that community that belongs to the social group categorized by the 11 factors 42 variables to define socio-economic vulnerabilities, then (ii) calculating the z-scores for each of the 11 factors 42 variables by using the overall mean and standard deviation per factor, and finally (iii) taking the sum of z-scores of all 11 factors 42 variables to account the total social vulnerability index of a specific region.

2.4. Social Equity Aspect

The concept of equity has been divided into two categories: (i) horizontal and (ii) vertical equity. Joseph et al. [2016] defined horizontal equity as the equal treatment of equals and vertical equity as unequal treatment of unequals. Horizontal equity could be expressed as each individual or group in the society being able to meet their needs since they have access to the same amount of resources separately. Vertical equity could be expressed as providing each individual or group in the society a varying amount of resources that is proportional with the level of their needs and vulnerabilities.

For horizontal equity, Cai [2008] studied a water delivery system from fiscal, social, economic, and environmental aspects to identify the required policy and reforms that ensure equal access of water among communities at all levels. Yan and Shih [2009] optimized the scheduling of emergency railroad repair such that the relief of multiple commodities to each location is equalized. Cao et al. [2016] optimized humanitarian relief distribution in a service network where meeting demand is considered for three different granularity including regional and national priorities.

For vertical equity, Thomopoulos et al. [2009] proposed a support tool to assist decision makers in differentiating their choice of equity perspectives and principles. Manaugh and El-

Geneidy [2012] developed a transportation network methodology that allows accessibility and less travel time for the varying socio-economic groups. Ogryczak et al. [2014] conducted a survey study for fair optimization methodology that is applied to the interdependent communication networks where these equitable models provide an unequal amount of system service based on operations-dependent relations. Zolfahri and Peyghaleh [2015] proposed a two-stage stochastic programming method for resource allocation for regional earthquake risk mitigation where the equity consideration led to variability in mitigation expenditures by geographic and structural vulnerability. Manaugh et al. [2015] evaluated the concept of equity and its integration into transportation network planning objectives and measures in terms of satisfying the various expectations of different social groups. Arnette and Zobel [2018] developed a risk-based optimization model to improve the disaster relief asset pre-positioning based on the varying residual risk measure of each location.

Chapter 3: Proposed Methodology

This developed research builds upon an initial multi-objective resilience-driven restoration optimization model proposed by Almogathawi et al. [2017]. This mixed-integer program maximizes the resilience of the interdependent infrastructure networks while minimizing the total cost associated with the restoration process. As for the contribution of this work, we extend how resilience is quantified by introducing a version of the SoVI-Lite score to account for a community resilience perspective. Additionally, a third objective for the existing work is formulated to represent social equity among the community. This extended model is an integration of a social vulnerability perspective on the restoration of interdependent infrastructure networks to introduce a community resilience-based component importance measure that ranks the critical components of interdependent infrastructure networks based on various social vulnerability variables.

3.1. Interdependent Infrastructure Network Restoration Model

3.1.1. Notation and Assumptions

In the multi-objective mixed-integer programming model that is extended for the interdependent infrastructure network restoration problem, the following assumptions hold: (i) there is no partial disruption in the nodes and links (hereafter, components) of the critical infrastructure networks through the disruption phase, (ii) there is no partial operability in the components of the critical infrastructure networks through the restoration phase, (iii) the required restoration duration differs for each component in the critical infrastructure networks, (iv) the amount of demand and supply is known for the nodes in the system, (v) the optimal amount of flow is known for each link in the system, (vi) the fixed unmet demand penalty cost (i.e., disruption cost) is assigned for each demand node in the networks, (vii) the varying restoration costs are assigned for each disrupted component in the networks, (viii) the varying unit flow cost that is

proportional with the length of the disrupted component is assigned to each link, (ix) the physical interdependency allows a component to be either fully operational or not operational based on the status of the components required for interdependency, and (x) known and fixed number of restoration crews are assigned to each network separately where each work crew can restore a single component at a given time through the restoration process. Most of these constraints which govern the component functionality, recoverability, disruption, and interdependency are loosened in the further studies so that they are represented by continuous states rather than binary stages.

Set K represents the set of infrastructure networks, and $T = \{1, \dots, \tau\}$ represents the set of available time periods for the restoration process. For each network $k \in K$, the sets of nodes and links are represented by N^k and L^k , respectively, where set of supply nodes and set of demand nodes are denoted by $N_s^k \subseteq N^k$ and $N_d^k \subseteq N^k$ respectively. The set of disrupted nodes are denoted by N'^k and the set of disrupted links are represented by L'^k . The maximum amount of supply at node $i \in N_s^k$ in network $k \in K$ is denoted by b_i^k , calculated as the maximum flow from node $i \in N_s^k$ to all demand nodes $i \in N_d^k$ in network $k \in K$. The amount of unmet demand at node $i \in N_d^k$ in network $k \in K$ at time $t \in T$ is represented with s_{it}^k . Thus, the total unsatisfied demand at all demand nodes in network $k \in K$ through the restoration process at time $t \in T$ is $\sum_{i \in N_d^k} s_{it}^k$. The unmet demand at demand node $i \in N_d^k$ in network $k \in K$ after the disruptive event is denoted by Q_i^k , and the equal weight of each network is represented by μ^k for network $k \in K$, such that $\sum_{k \in K} \mu^k = 1$.

The cost of restoration of disrupted nodes and links in network $k \in K$ are represented as fn_i^k for $i \in N'^k$ and fl_{ij}^k for $(i, j) \in L'^k$, respectively. The unitary unsatisfied demand cost associated with node $i \in N_d^k$ is represented with p_i^k , while the unitary flow cost through link

$(i, j) \in L^k$ is represented with c_{ij}^k . The binary variable z_i^k is equal to 1 if node $i \in N^k$ is restored and 0 otherwise. Likewise, binary variable y_{ij}^k is equal to 1 if link $(i, j) \in L^k$ is restored and 0 otherwise. The total flow through link $(i, j) \in L^k$ in network $k \in K$ and at time $t \in T$ is represented by non-negative variable x_{ijt}^k .

The restoration duration for node $i \in N^k$ and for link $(i, j) \in L^k$ are denoted by dn_i^k and dl_{ij}^k that are proportional to the capacity of the nodes and length of the links in the networks, respectively. The flow capacity for link $(i, j) \in L^k$ in network $k \in K$ is u_{ij}^k . The binary variable β_{it}^k is equal to 1 if the node $i \in N^k$ is operational and 0 otherwise, and the binary variable α_{ijt}^k is equal to 1 if the link $(i, j) \in L^k$ is operational and 0 otherwise in network $k \in K$ at time $t \in T$. The set of available work crews or resources for the restoration process of each network $k \in K$ is represented with R^k , where the resources are assigned specifically for each network in terms of the required skills and expertise. γ_{it}^{kr} and δ_{ijt}^{kr} represent the scheduling variables for node $i \in N^k$ and link $(i, j) \in L^k$ in network $k \in K$ and at time $t \in T$, respectively. These variables are both equal to 1 if the restoration of the associated disrupted component is completed by work crew $r \in R^k$ at time $t \in T$ and 0 otherwise. Finally, the network interdependencies are represented by $((i, k), (\bar{i}, \bar{k})) \in \Psi$, where node $\bar{i} \in N^{\bar{k}}$ in network $\bar{k} \in K$ is physically dependent to node $i \in N^k$ in network $k \in K$ in terms of functionality.

3.1.2. Community Resilience Measures

In this research, the social vulnerability index is introduced into the optimization model by defining a parameter $SoVI_i^k$, which represents an index between 0 (socially the least vulnerable) and 1 (socially the most vulnerable) for demand node $i \in N_d^k$ in network $k \in K$. The value of $SoVI_i^k$ is calculated by the SoVI-Lite method separately for each demand node according to the

geographical region it represents. Furthermore, the obtained social vulnerability indices could be standardized to be scaled between 0 and 1 where 1 represents socially the most vulnerable community and 0 stands for socially the most resilient community. The standardization formula for the social vulnerability index of a specific community z , where $z \in X$ and X is the set of all social vulnerability indices, can be seen in Eq.(1). By standardization, any negative social-vulnerability scores would be avoided without changing the probability distribution and it would be integrated in the proposed optimization model without conflicting with the adopted resilience metric and total recovery cost formulation.

$$\frac{z - \min(X)}{\max(X) - \min(X)}, \quad \forall z \in X \quad (1)$$

Moreover, to give relatively more emphasis on the regional areas that are assigned with higher social vulnerability indices (i.e., 0.7 and higher values of $SoVI_i^k$), this research introduces the exponential formulation of social vulnerability scores, which is represented as V_i^k , as in Eq. (2). Hence, with this formulation we highly penalize the increases in the social vulnerability scores for more vulnerable areas. Thus, the penalty of an increase in the vulnerability level would be represented more drastically in the proposed method, since the relative importance of different social vulnerability scores would become exponential rather than linear ratios. The constant a in Eq. (2) is chosen such a way that it would generate a reasonable emphasize on the higher social vulnerability scores without causing computational delays.

$$V_i^k = e^{a \times SoVI_i^k}, \quad \forall i \in N_d^k, a \in Z^+ \quad (2)$$

Additionally, the parameter P_i^k is introduced to indicate the population density of the geographical region in which the demand node is located to account for human occupancy levels in our resilience-driven objective. In addition to SoVI-driven measures of social vulnerability, the

size of the population being served by infrastructure demand nodes can also be considered as a perspective of community -resilience. The formulation to represent the population density served by demand node $i \in N_d^k$ is shown in Eq. (3).

$$P_i^k = \frac{\text{population of the service area served by demand node } i}{\text{total population of all service areas}}, \quad \forall i \in N_d^k \quad (3)$$

3.1.3. Optimization Model

The complete version of our proposed optimization model with the focus of two objective functions to (i) maximize the resilience for a set of interdependent infrastructure networks and (ii) minimize the total cost associated with the restoration process is as follows. These two conflicting objectives and the constraints defined through the development of our model are explained in a more detailed way in this section.

We measure resilience as a function of unmet demand s_{it}^k , for demand node $i \in N_d^k$ in network $k \in K$ through recovery at time $t \in T$, where increase in the slack demand represents the loss in the maximum flow due to a disruption as seen in Eq. (4). The loss in demand at demand node $i \in N_d^k$ in network $k \in K$ is denoted by Q_i^k , and $\sum_{i \in N_d^k} Q_i^k$ measures the total unmet demand in network $k \in K$ after the disruption and before the recovery commences. In this case, $\sum_{i \in N_d^k} Q_i^k$ represents the maximum amount of unmet demand in the infrastructure network, and it is assumed network performance cannot exceed its original value after recovery. Further, we introduce the importance of demand nodes from a community resilience perspective with parameters V_i^k and P_i^k for demand node $i \in N_d^k$ in network $k \in K$, representing social vulnerability and population density, respectively. Recovery is represented as the difference in the total unmet demand just before and at time t during the restoration process. Thus, in the resilience objective function

$\sum_{k \in K} \left(\sum_{i \in N_d^k} (Q_i^k V_i^k P_i^k) - \sum_{i \in N_d^k} (s_{it}^k V_i^k P_i^k) \right)$ denotes the amount of slack restored during the restoration process. Reducing the total amount of unmet demand means increasing the flow that has been carried through the interdependent infrastructure network, thus increasing the performance of the interdependent networks. Hence, improving the effectiveness of the infrastructure network and its ability to recover the maximum amount of possible slack through the recovery, given the prioritization of the demand nodes according to the social vulnerability scores and population densities of the region they represent is accomplished through the restoration process, is denoted in the resilience objective in Eq. (4).

$$\max \sum_{k \in K} \mu^k \sum_{t=1}^{\tau} \left(\frac{t \left[\sum_{i \in N_d^k} (Q_i^k V_i^k P_i^k) - \sum_{i \in N_d^k} (s_{it}^k V_i^k P_i^k) \right] - (t-1) \left[\sum_{i \in N_d^k} (Q_i^k V_i^k P_i^k) - \sum_{i \in N_d^k} (s_{i(t-1)}^k V_i^k P_i^k) \right]}{\sum_{i \in N_d^k} (\tau Q_i^k V_i^k P_i^k)} \right) \quad (4)$$

For the cost objective in Eq. (5), we consider three different cost categories that are associated with the restoration process of the system. The flow cost, c_{ij}^k , represents the unitary cost of carrying flow through link $(i, j) \in L^k$ in network $k \in K$ in the system. The varying restoration costs, fn_i^k for node $i \in N^k$ and fl_{ij}^k for link $(i, j) \in L^k$ denotes the cost associated with the available resources and their utilization in the restoration process of disrupted components where these costs are proportional to the supply capacity of the nodes and the length of the links in the networks. Finally, the disruption cost p_i^k for node $i \in N_d^k$ quantifies the penalty cost for unmet demand due to the disruptive event. Additionally, we assign social vulnerability scores and population densities to penalty costs for disrupted demand nodes. In the objective, $\sum_{k \in K} \sum_{i \in N_d^k} (p_i^k s_{it}^k V_i^k P_i^k)$ assumes that to recover the exact same amount of slack demand from the socially more vulnerable and denser areas, the amount of required economic investments increases to meet the same resilience levels when it is compared with socially less vulnerable and less populated areas [Cutter et al. 2003]. Hence, minimizing the cost objective of our model also

considers the recovery of all demand nodes that are associated with highly vulnerable and more populated regions to support the community resilience perspective.

$$\min \sum_{k \in K} \left(\sum_{i \in N^k} f n_i^k z_i^k + \sum_{(i,j) \in L^k} f l_{ij}^k y_{ij}^k + \sum_{t \in T} \left[\sum_{(i,j) \in L^k} c_{ij}^k x_{ij}^k + \sum_{i \in N_d^k} p_i^k s_{it}^k V_i^k P_i^k \right] \right) \quad (5)$$

The two objectives above are balanced for the following constraints.

$$\sum_{(i,j) \in L^k} x_{ijt}^k \leq b_i^k, \quad \forall i \in N_s^k, k \in K, t \in T \quad (6)$$

$$\sum_{(i,j) \in L^k} x_{ijt}^k - \sum_{(j,i) \in L^k} x_{jit}^k = 0, \quad \forall i \in N^k \setminus \{N_s^k, N_d^k\}, k \in K, t \in T \quad (7)$$

$$\sum_{(j,i) \in L^k} x_{jit}^k + s_{it}^k = b_i^k, \quad \forall i \in N_d^k, k \in K, t \in T \quad (8)$$

$$x_{ijt}^k - u_{ij}^k \leq 0, \quad \forall (i,j) \in L^k, k \in K, t \in T \quad (9)$$

$$x_{ijt}^k - u_{ij}^k \beta_{it}^k \leq 0, \quad \forall (i,j) \in L^k, i \in N^k, k \in K, t \in T \quad (10)$$

$$x_{ijt}^k - u_{ij}^k \beta_{jt}^k \leq 0, \quad \forall (i,j) \in L^k, j \in N^k, k \in K, t \in T \quad (11)$$

$$x_{ijt}^k - u_{ij}^k \alpha_{ijt}^k \leq 0 \quad \forall (i,j) \in L^k, k \in K, t \in T \quad (12)$$

$$\beta_{it}^{\bar{k}} - \beta_{it}^k \leq 0, \quad \forall ((i,k), (\bar{i}, \bar{k})) \in \Psi, t \in T \quad (13)$$

$$y_{ij}^k = \sum_{r \in R^k} \sum_{t \in T} \delta_{ijt}^{kr}, \quad \forall (i,j) \in L^k, k \in K \quad (14)$$

$$z_i^k = \sum_{r \in R^k} \sum_{t \in T} \gamma_{it}^{kr}, \quad \forall i \in N^k, k \in K \quad (15)$$

$$\alpha_{ijt}^k \leq \sum_{r \in R^k} \sum_{l=1}^t \delta_{ijl}^{kr}, \quad \forall (i,j) \in L^k, k \in K, t \in T \quad (16)$$

$$\beta_{it}^k \leq \sum_{r \in R^k} \sum_{l=1}^t \gamma_{il}^{kr}, \quad \forall i \in N^k, k \in K, t \in T \quad (17)$$

$$\sum_{(i,j) \in L^k} \sum_{l=t}^{\min(\tau, t+dl_{ij}^k-1)} \delta_{ijl}^{kr} \quad \forall k \in K, r \in R^k, t \in T \quad (18)$$

$$+ \sum_{i \in N^k} \sum_{l=t}^{\min(\tau, t+dn_i^k-1)} \gamma_{il}^{kr} \leq 1,$$

$$\sum_{t=1}^{dl_{ij}^k-1} \alpha_{ijt}^k = 0, \quad \forall (i,j) \in L^k, k \in K \quad (19)$$

$$\sum_{t=1}^{dn_i^k-1} \beta_{it}^k = 0 \quad \forall i \in N^k, k \in K \quad (20)$$

$$\sum_{r \in R^k} \sum_{t=1}^{dl_{ij}^k-1} \delta_{ijt}^{kr} = 0, \quad \forall (i,j) \in L^k, k \in K \quad (21)$$

$$\sum_{r \in R^k} \sum_{t=1}^{dn_i^k-1} \gamma_{it}^{kr} = 0, \quad \forall i \in N^k, k \in K \quad (22)$$

$$s_{it}^k \geq 0, \quad \forall i \in N_d^k, k \in K, t \in T \quad (10)$$

$$x_{ijt}^k \geq 0, \quad \forall (i,j) \in L^k, k \in K, t \in T \quad (11)$$

$$y_{ij}^k \in \{0,1\}, \quad \forall (i,j) \in L^k, k \in K \quad (25)$$

$$z_i^k \in \{0,1\}, \quad \forall i \in N^k, k \in K \quad (26)$$

$$\alpha_{ijt}^k \in \{0,1\}, \quad \forall (i,j) \in L^k, k \in K, t \in T \quad (27)$$

$$\beta_{it}^k \in \{0,1\}, \quad \forall i \in N^k, k \in K, t \in T \quad (28)$$

$$\delta_{ijt}^{kr} \in \{0,1\}, \quad \forall (i,j) \in L^k, k \in K, t \in T, r \in R^k \quad (29)$$

$$\gamma_{it}^{kr} \in \{0,1\}, \quad \forall i \in N^k, k \in K, t \in T, r \in R^k \quad (30)$$

The first set of constraints, Eqs. (6)-(8), govern the flow conservation of node $i \in N^k$. Constraints (9)-(12) control the capacity of disrupted and undisrupted components, where Eq. (9) considers undisrupted links, Eqs. (10) and (11) consider the disrupted nodes, and Eq. (12) considers disrupted links. Constraint (13) governs the physical interdependency between nodes to ensure that node $\bar{i} \in N^{\bar{k}}$ in network $\bar{k} \in K$ is operational at time $t \in T$ only if the node $i \in N^k$ in network $k \in K$ is also operational at time $t \in T$. Constraints (14)-(22) represent the assignment scheduling for the restoration process of disrupted components, where Eqs. (14) and (15) ensure the work crew assignment for the disrupted components if their restoration is a must, Eqs. (16) and (17) ensure the operability of a component when its restoration is completed by the specifically assigned work crew $r \in R^k$, Eq. (18) ensures that a single work crew can restore at most one disrupted component (either a link or a node) in network $k \in K$ at a specific time $t \in T$, and Eqs. (19)-(22) ensure that for a disrupted component to be functional, its restoration should be completed by the assigned work crew. Finally, constraints (103)-(30) indicate the nature of decision variables in the optimization model.

3.2. Resilience-Driven Component Importance Measure

3.2.1. Notation and Assumptions

In the multi-objective mixed-integer programming model that is extended for integrating the resilience-driven CIM with the interdependent infrastructure network restoration problem, the same assumptions and model notation hold with the previously discussed optimization model. Differently, the weight of each critical infrastructure network is represented by w^k for network $k \in K$ where $\sum_{k \in K} w^k = 1$ in this part of the research.

3.2.2. Social Vulnerability Measures

The community resilience perspective is introduced into the interdependent infrastructure network restoration model that is integrated with the resilience-driven component importance measure, by defining a parameter, $SoVI_{ic}^k$ for each demand node $i \in N_d^k$ in network $k \in K$ for social vulnerability variable $c \in C$, where this parameter represents an index between 0 and 1. The value of $SoVI_{ic}^k$ is calculated separately for social vulnerability variable $c \in C$ according to the SoVI-Lite algorithm [Cutter et al. 2013, Evans et al. 2014] with the same steps in previously explained community resilience part of this research. The only difference is that the z-scores of the multiple social vulnerability variables is not summed since the social vulnerability indices are calculated separately for each social vulnerability variable $c \in C$. The standardization of the social vulnerability indices as in Eq. (1) is applied on each social vulnerability variable separately. Additionally, the exponential formulation for each social vulnerability variable index is adopted as in Eq. (3112) and the population density is included in the model as the same measure in Eq. (3).

$$V_{ic}^k = e^{a \times SoVI_{ic}^k}, \quad \forall i \in N_d^k, a \in Z^+ \quad (3112)$$

3.2.3. Optimization Model

The extended optimization model that considers social equity and resilience-driven CIM contains three objective functions: (i) to maximize the resilience of the set of interdependent infrastructure networks, (ii) to minimize the total cost associated with the restoration of these critical infrastructure networks, and (iii) to plan the recovery schedule of the disrupted communities according to the vertical social equity distribution among them. The resilience maximization and total cost minimization objectives are same as the previously discussed multi-objective resilience-driven mixed-integer interdependent infrastructure network restoration model.

The only difference is that the social vulnerability scores are included separately for each social vulnerability variable for both resilience maximization and total cost minimization objectives as in Eq. (32) and Eq. (33), respectively.

$$\max \sum_{k \in K} \mu^k \sum_{t=1}^{\tau} \left(\frac{t [\sum_{i \in N_d^k} (Q_i^k V_i^k P_i^k) - \sum_{i \in N_d^k} (s_{it}^k V_i^k P_i^k)] - (t-1) [\sum_{i \in N_d^k} (Q_i^k V_i^k P_i^k) - \sum_{i \in N_d^k} (s_{i(t-1)}^k V_i^k P_i^k)]}{\sum_{i \in N_d^k} (\tau Q_i^k V_i^k P_i^k)} \right) \quad (32)$$

$$\min \sum_{k \in K} \left(\sum_{i \in N^k} f n_i^k z_i^k + \sum_{(i,j) \in L^k} f l_{ij}^k y_{ij}^k + \sum_{t \in T} \left[\sum_{(i,j) \in L^k} c_{ij}^k x_{ij}^k + \sum_{i \in N_d^k} p_i^k s_{it}^k V_{ic}^k P_i^k \right] \right) \quad (33)$$

To account for social equity, we incorporate both horizontal and vertical equity concepts for network restoration planning. Horizontal equity is introduced in the first two objectives by ensuring that demand of all disrupted communities is met in the system. To account for vertical equity, a third objective is formulated to guide the restoration process to start with more heavily disrupted communities. To achieve this, the resilience of each demand node $i \in N_d^k$ at each time t is calculated as $\frac{t(Q_i^k - s_{it}^k) - (t-1)(Q_i^k - s_{i(t-1)}^k)}{\tau(Q_i^k)}$, and the resilience residual of each demand node is measured by subtracting the demand node resilience at time t from the optimal resilience level of 1. Then the total system residual through the duration of complete restoration is minimized. Additionally, to emphasize more heavily on the vertical equity, the demand node residual at each time t is weighted with social vulnerability score, V_{ic}^k , and population density, P_i^k , of the effected community. The social equity-motivated objective is formulated in Eq. (14).

$$\min \sum_{t \in T} \left(\sum_{i \in N_d^k} \left(\left(1 - \frac{t(Q_i^k - s_{it}^k) - (t-1)(Q_i^k - s_{i(t-1)}^k)}{\tau(Q_i^k)} \right) V_{ic}^k P_i^k \right) \right) \quad (14)$$

The complete optimization model is same as the previously discussed one where to provide the horizontal equity in the system, the following two constraints are added to the model. Eqs. (3515) and (3616) ensure that all disrupted components would be restored hence, the unmet demand in each community that is represented by demand nodes is satisfied fully.

$$\sum_{r \in R^k} \sum_{t=1}^{\tau} \delta_{ijt}^{kr} = 1, \quad \forall (i, j) \in L^k, k \in K \quad (3515)$$

$$\sum_{r \in R^k} \sum_{t=1}^{\tau} \gamma_{it}^{kr} = 1, \quad \forall i \in N^k, k \in K \quad (3616)$$

3.2.4. Component Importance Measure

A resilience-based component importance measure, Optimal Recovery Time (ORT), an extension (to multiple interdependent infrastructure networks) of a CIM introduced by Fang et al. [2016] is utilized. ORT is defined as the optimal time to recover a disrupted component such that the resilience of the interdependent infrastructure networks is maximized over the recovery time horizon [Almoghathawi et al. 2017]. The ORT measure prioritizes the disrupted components, both the nodes and links, with the higher impact on the resilience of the interdependent infrastructure networks and schedules the restoration process accordingly. With this CIM, decision makers can rank the disrupted components according to their latest restoration completion time through the available restoration duration. The earlier the disrupted component is scheduled for restoration, a higher importance is assigned to it, and thus, the critical components of the interdependent infrastructure networks would be scheduled for restoration, since they have a higher impact on the resilience of the networks. The formal definition and the mathematical formulation of the ORT component importance measure is located below.

The ORT of a disrupted component $e \in E'^k = N'^k \cup L'^k$ in network $k \in K$ is represented as I_e^{ORT} , as shown in Eqs. (3717) and (3818). In the formulation, μ_{et}^k denotes the operability status of component μ_{et}^k in network $k \in K$ at time $t \in T$. If μ_{et}^k is equal to 1, then the disrupted component is operational at time $t \in T$ and 0 otherwise.

$$I_e^{ORT} = 1 + \sum_{t \in T} (1 - \mu_{et}^k) \quad (3717)$$

where

$$\mu_{et}^k = \begin{cases} z_{it}^k, & \text{if } e \text{ is a node, } e = i \\ y_{ijt}^k, & \text{if } e \text{ is a link, } e = (i, j) \end{cases} \quad (3818)$$

3.2.5. Multi-criteria Decision Analysis Technique for Aggregated Ranking

Multi-criteria decision analysis (MCDA) techniques are particularly useful for aiding in selecting from one of several discrete alternatives when several criteria are being considered [Lootsma 1999]. In this study, we utilize the Technique for Order Preferences by Similarity to an Ideal Solution (TOPSIS), which ranks alternatives that balance closeness to the best solution and distance from the worst [Hwang and Yoon 1981]. Sets $A = \{A_e | e = 1, \dots, n\}$ and $C = \{C_c | c = 1, \dots, m\}$ denote respectively the set of possible alternatives and criteria, respectively. Additionally, $Y = \{y_{ec} | e = 1, \dots, n; c = 1, \dots, m\}$ denotes the set of performance scores of the alternatives for each criterion. Finally, $\omega = \{\omega_c | c = 1, \dots, m\}$ denotes the set of criteria weights, where $\omega_c \geq 0$ and $\sum_{c=1}^m \omega_c = 1$ such that larger value of ω_c suggests that criterion c is more important to the decision maker. Eq. (3919) is defined to scale the performance scores of the alternatives, as often criteria are measured on different scales. Eq. (40) represents how the criteria weights are assigned to the scaled aggregation scores in TOPSIS.

$$r_{ec}(y) = \frac{y_{ec}}{\sqrt{\sum_{e=1}^n y_{ec}^2}}, \quad e = 1, \dots, n; \quad c = 1, \dots, m \quad (3919)$$

$$v_{ec}(y) = \omega_c r_{ec}(y), \quad e = 1, \dots, n; \quad c = 1, \dots, m \quad (40)$$

In the next step, the positive ideal solution, A^+ , and the negative ideal solution, A^- , are determined by the collection of most preferred and the least preferred weighted and scaled aggregation score, v_{ec} , for each criterion, respectively. Eqs. (4120) and (421) represent the formula for finding the PIS and NIS respectively, where C^+ represents the set of benefit criteria and C^- represents the cost criteria.

$$A^+ = \{v_1^+(y), \dots, v_m^+(y)\} = \left\{ \left(\max_{l \leq e \leq n} v_{ec}(y) \mid c \in C^+ \right), \left(\min_{l \leq e \leq n} v_{ec}(y) \mid c \in C^- \right) \right\} \quad (4120)$$

$$A^- = \{v_1^-(y), \dots, v_m^-(y)\} = \left\{ \left(\min_{l \leq e \leq n} v_{ec}(y) \mid c \in C^+ \right), \left(\max_{l \leq e \leq n} v_{ec}(y) \mid c \in C^- \right) \right\} \quad (421)$$

Next, the distance, D_e^+ , between alternative A_e and the positive ideal solution is calculated with Euclidean distance in Eq. (40). Similarly, the distance, D_e^- , between the same alternative, A_e and the negative ideal solution is found in Eq. (4120). Finally, the balance between positive and negative ideal solutions is calculated with Eq. (421), where higher S_e^+ values suggest a higher similarity to the positive ideal solution. A ranking of alternatives could be produced from an ordering of highest to lowest S_e^+ values.

$$D_e^+ = \sqrt{\sum_{c=1}^m [v_{ec}(y) - v_c^+(y)]^2}, \quad e = 1, \dots, n \quad (43)$$

$$D_e^- = \sqrt{\sum_{c=1}^m [v_{ec}(y) - v_c^-(y)]^2}, \quad e = 1, \dots, n \quad (44)$$

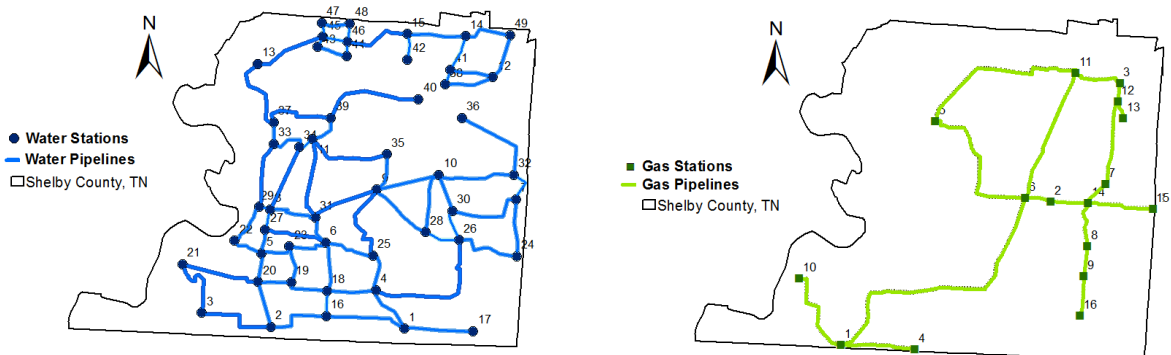
$$S_e^+ = \frac{D_e^-}{D_e^+ + D_e^-}, \quad e = 1, \dots, n \quad (45)$$

In this study, the set of alternatives, A , are the disrupted components of the critical infrastructure networks and the set of criteria, C , are the multiple social vulnerability variables. The performance scores of the alternatives over each criteria, v_{eC} , are the rank of the disrupted components in the restoration schedule of interdependent infrastructure networks that are based on each social vulnerability variable independently.

Chapter 4: Illustrative Example

4.1. Interdependent Infrastructure Network Restoration

The community resilience-driven interdependent infrastructure network restoration model is applied with data describing interdependent networks in Shelby County, Tennessee, whose location in the New Madrid Seismic Zone makes it susceptible to earthquake risk [González et al. 2016]. We consider three interdependent infrastructure networks: water, natural gas, and electric power distribution systems. Figure 3 depicts the geographical layout of the infrastructure networks independently and with the consideration of their physical interdependency. The interdependent infrastructure networks consist of a total of 125 nodes including 15 demand nodes in the water network, 13 demand nodes in the gas network, and 9 demand nodes in the power network. There are total of 176 bi-directional links from all three infrastructure networks.



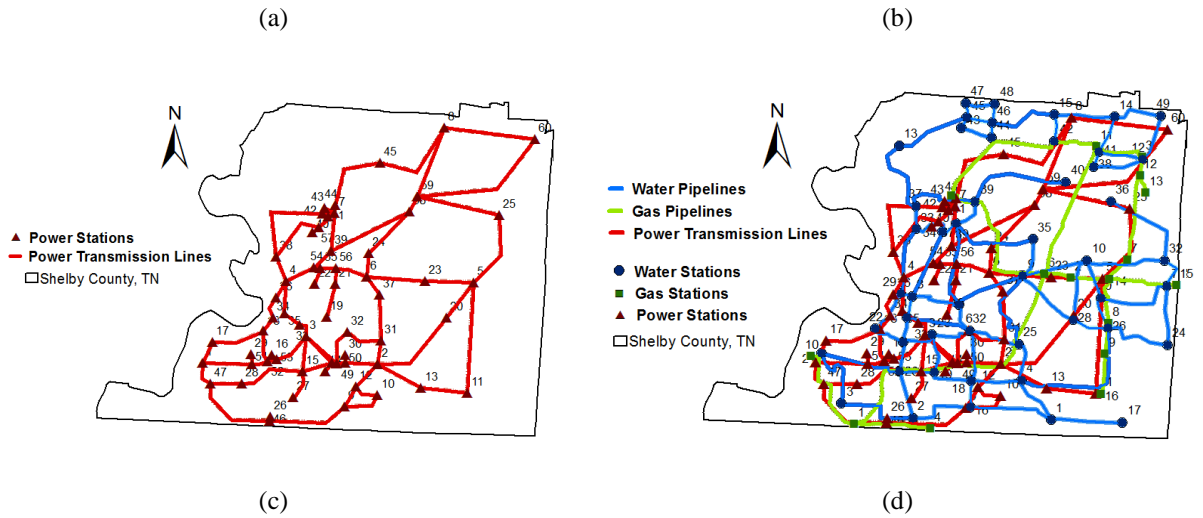


Figure 3. Critical (a) water, (b) gas, and (c) power infrastructure networks of Shelby County, TN and (d) their physical interdependencies respectively (adapted from González et al. [2016]).

4.1.1. Social Vulnerability in Shelby County, TN

The SoVI-Lite algorithm [Cutter et al. 2013, Evans et al. 2014] is adapted to calculate the social vulnerability indices of the demand nodes from the critical infrastructure networks in Shelby County, TN. Most of the 11 factor groups in Table 1 are addressed by the available 14 socio-economic variables listed in Table 2.

Table 2. Percentage based district-level social vulnerability variables available in Shelby County, TN data for the SoVI-Lite algorithm.

Households earning under \$75,000 annually	Population that is Asian
Population under the age of 5	Single-female households
Households living below the poverty line	Population without a high school education
Households requiring food stamps	Population working in low-skilled service jobs
Population over the age of 65	Population that is unemployed

Population that is Hispanic	Population speaking English as a second language
Population that is African-American	Population that is female

An initial study by Barker et al. [2018] explored the 14 variables for five different geographical districts in Shelby County. Figure 4 illustrates the correlation among these 14 variables that are listed in Table 2, calculated using the Pearson correlation coefficient. Figure 4 suggests that among these 14 variables, the intersection of with a high positive correlation (Pearson correlation coefficient $r \geq 0.85$) is visualized with dark blue. As the positive correlation decreases, the dark blue color becomes lighter. For example, the variable “75000” which stands for the percentage of household that earns less than \$75,000 annually has a high positive correlation ($r \geq 0.85$) with the variable “African-American,” “Single Female,” “No Diploma,” “Food Stamp,” “Poverty,” and “Unemployed,” where these variables stand for the percentage of the population that is African-American, percentage of single-female households in the society where the existence of spouse is missing, percentage of the population that did not graduate from high-school, percentage of the households that requires social security relief such as food stamps, percentage of the households that lives under the poverty line, and percentage of the population that is unemployed, respectively. On the contrary, the intersection of the variables that have a high negative correlation, where the Pearson correlation coefficient is below a certain value ($r \leq -0.85$), is shaded with dark red and as the negative correlation decreases, the dark red color becomes lighter. As an example, the variable “Asian,” which represents the percentage of population that is Asian, has a high negative correlation ($r \leq -0.85$) with the previously

explained variables “African-American,” “Single Female,” “No Diploma,” “Food Stamp,” “Poverty,” and “Unemployed.”

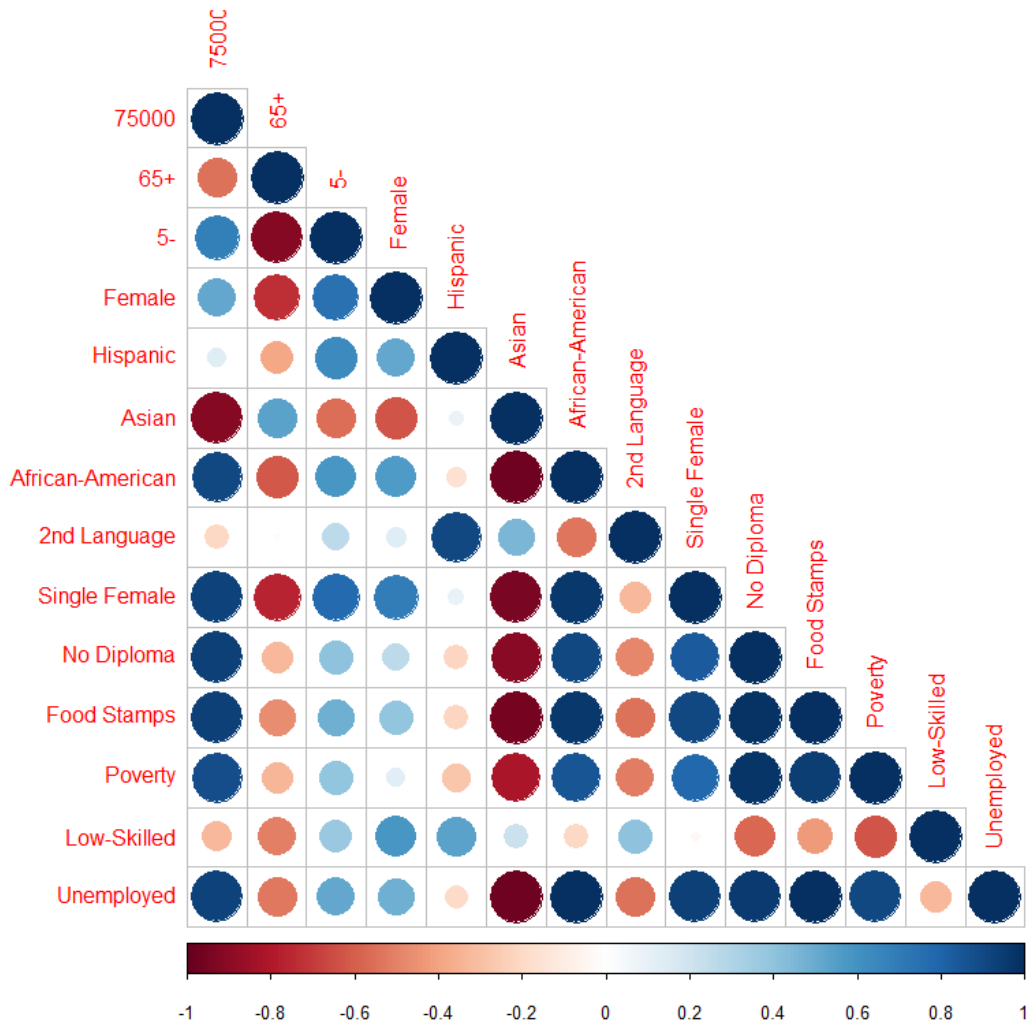


Figure 4. An illustration of the correlation analysis between the 14 social vulnerability variables available for the district level in Shelby County, TN, where darker red color and bigger circle size represent a higher negative correlation and darker blue color and bigger circle size represent a higher positive correlation.

In this research, to provide a higher level of granularity for social vulnerability in Shelby County, SoVI-Lite indices are calculated at the block group level rather than the district level. A block group is a statistical division of census tracts that consists of clusters of blocks and generally contain between 600 and 3,000 people who are the residents of the covered contiguous area [U.S.

Census Bureau 2010]. There are 621 block groups making up Shelby County, which consists in a total of 928,794 residents. These numbers are the exact values that are utilized through the social vulnerability calculations with respect to the availability of data where around 10 block groups that contain around 4,000 citizens are eliminated because of the missingness of certain required demographics. However, not all 14 variables are available at the block group level either. Figure 5 highlights the correlation among the eight variables available in the block group level of Shelby County, and it appears that all of the existing variables have a lower positive and negative correlation between each other when compared with the district level data. However, in the block group level data, none of the two-variable combinations have a high correlation (neither positive nor negative) behavior especially when the correlation measures in the district level are considered. In the block group level, the highest positive correlation is between the variable “75000,” and the variables “African-American,” “Single Female,” and “Poverty,” but the Pearson correlation coefficient has a lower value ($r \leq 0.6$). The definition of these variables is exactly the same with the district level variables. On the other hand, in the block group level data, none of the variable pairs end up with a Pearson correlation coefficient value that is below a certain value ($r \leq -0.6$), thus there does not exist any high negative correlation among these variables either.

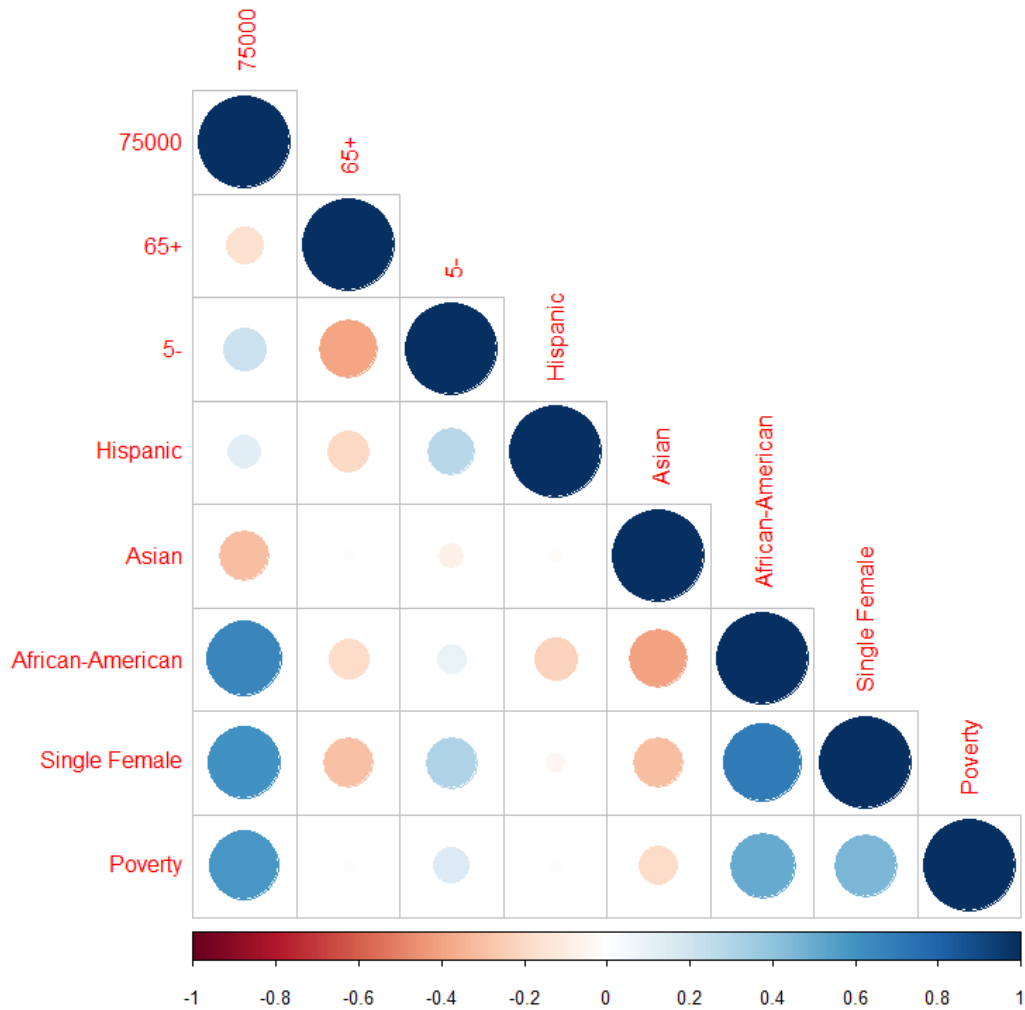


Figure 5. An illustration of the correlation analysis with the available social vulnerability variables in the block group level in Shelby County, TN, where darker red color and bigger circle size represent a higher negative correlation and darker blue color and bigger circle size represent a higher positive correlation.

As such, for the block group data, all the existing variables are included in the social vulnerability calculations. Additionally, as some variables that exist in the district level data but not in the block group level data are also covered by the above analysis. For example, in the district level data, the variable “75000” and “African-American” have highly positive correlation with the variables “No Diploma,” “Food Stamp,” and “Unemployment.”. As such, the existence of these two variables in the block group data provides insight into the three missing variables and complements the information provided with only two variables. Thus, to not lose any information,

the set of all eight variables are considered in this study, as enumerated in Table 3. The SoVI-Lite calculations are based on these eight variables which contain neither high positive nor high negative correlation.

Table 3. The percentage based social vulnerability variables that are utilized through the SoVI-Lite algorithm for the block group level in Shelby County, TN.

Households earning under \$75,000 annually	Population that is Hispanic
Population over the age of 65	Population that is African-American
Population that is Asian	Single-female based households
Population under the age of 5	Households that are in poverty

To assign social vulnerability scores, V_i^k , and population densities, P_i^k , to demand nodes at the block level, specific geographical regions were identified to represent each demand node. To estimate the geographical region that each demand node covers, Voronoi diagrams [Okabe et al. 2008] are utilized. In essence, the Voronoi diagram method can be summarized as follows: for a given finite set of points $\{p_1, \dots, p_n\}$ in the Euclidean plane, X , the Voronoi cell Vor_k contains the point p_k and all the other points whose distance to p_k , $d(p_x, p_k)$, is less than their distance to any other point, p_j , $d(p_x, p_j)$. The more formal and general definition is formulated in Eq. (46).

$$Vor_i = \{p \mid d(p, p_i) \leq d(p, p_j)\}, \quad \forall j \neq i, j = 1, \dots, n \quad (46)$$

In this study, each demand node from all three infrastructure networks in Shelby County is considered as the Voronoi seeds and the coverage areas of the demand nodes are represented by the Voronoi cells in which they are located. These Voronoi cells, along with their associated block groups, are represented in Figure 6**Error! Reference source not found.** The social vulnerability indices of all the block groups that are either fully or partially included in the single Voronoi cell

are assigned to the demand node that is considered as the seed of the region. The population densities are however assigned proportionally to the demand nodes according their portion that is included in each Voronoi region (i.e., for a block group that is divided into two by the border of two neighbor cells, its social vulnerability index is assigned to both demand nodes, but its population is divided into two and assigned proportionally to each demand node separately).

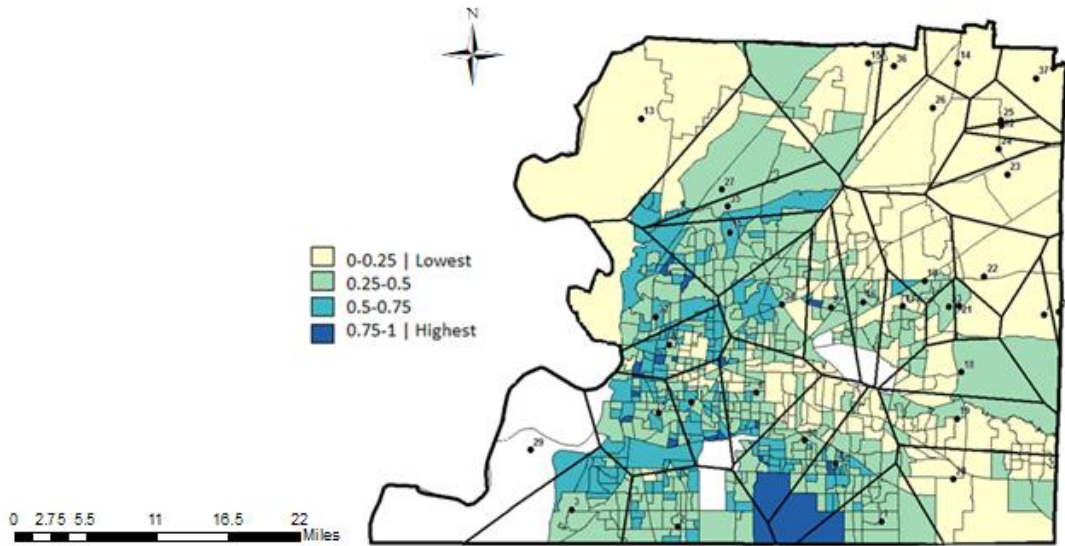


Figure 6. An illustration of the distribution of block groups into Voronoi cells that are created by the demand nodes of three critical infrastructure networks in Shelby County, TN.

The social vulnerability indices of the demand nodes are calculated by taking the average of the social vulnerability indices of the included block groups in the same Voronoi cell. Figure 7 represents the social vulnerability indices, $SoVI_i^k$, of all the demand nodes in critical infrastructure networks of Shelby County. Figure 8 illustrates the exponential representation of the social vulnerability scores, V_i^k , that are included in the optimization model to give relatively higher importance to the demand nodes in more vulnerable areas. For example, according to these figures, demand nodes 32, 5, 8, 3 and 11 represent areas that may require prior and more resources to ensure their timely restoration. Additionally, Figure 9 represents the exponential social

vulnerability scores, V_i^k , of the demand nodes in Shelby County to illustrate which demand nodes serve socially more vulnerable areas. The block groups that are colored white represent a lack of household information or a lack of residents.

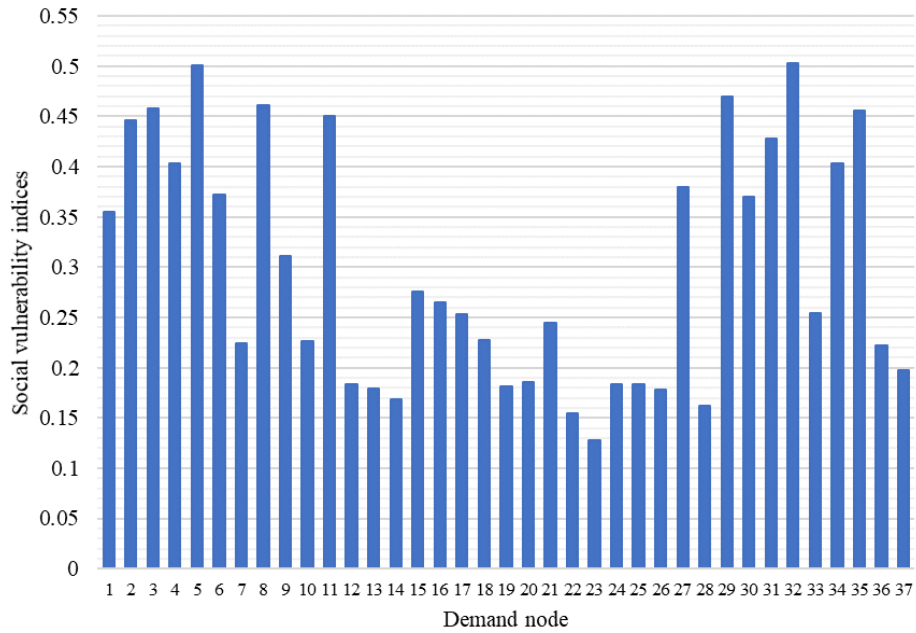


Figure 7. Illustration of social vulnerability indices, $SoVI_i^k$ of the demand nodes.

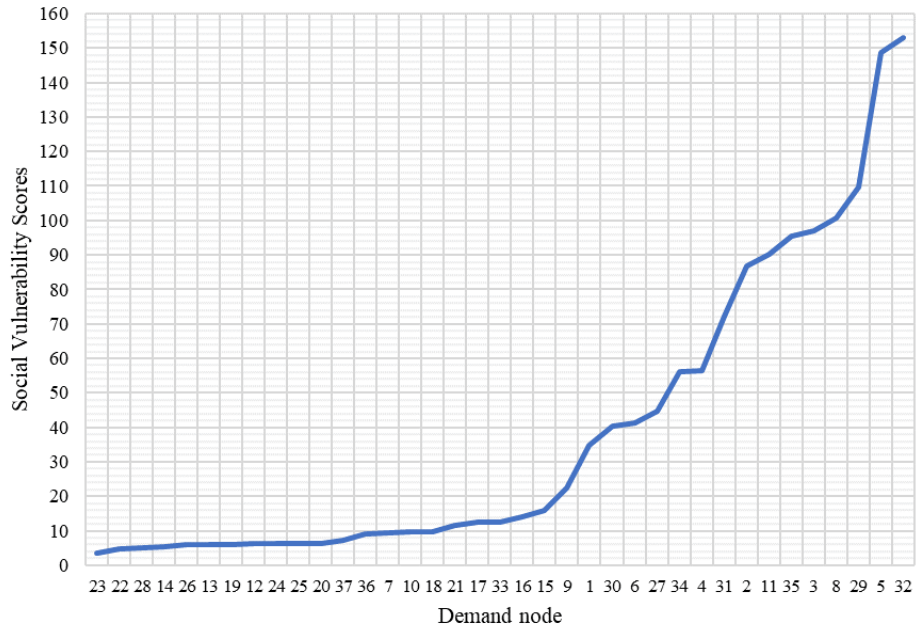


Figure 8. Illustration of the exponential social vulnerability scores, V_i^k .

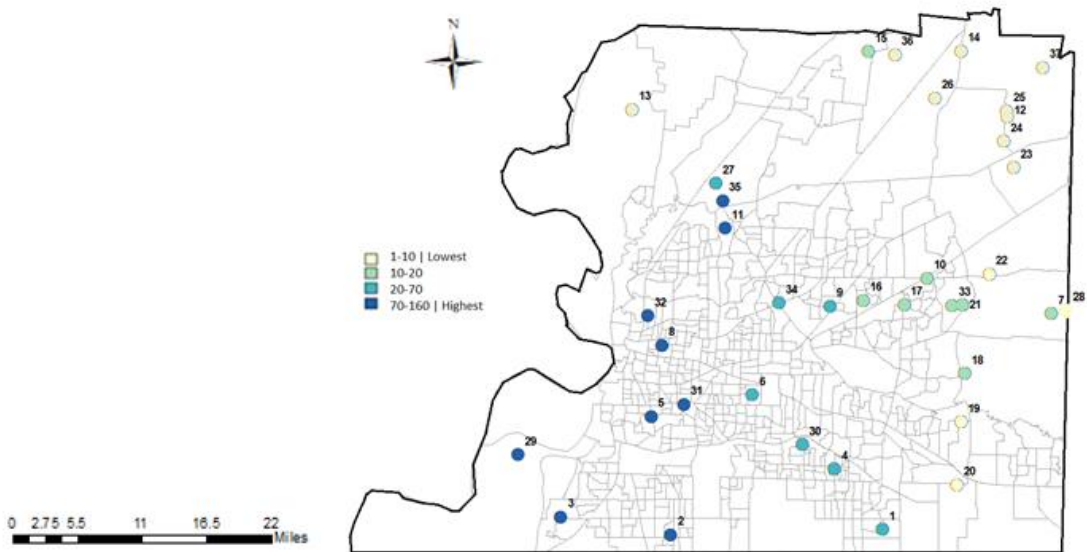


Figure 9. Representation of the exponential social vulnerability scores, V_i^k , of the demand nodes of all three critical infrastructure networks over Shelby County, TN.

The multi-objective problem is solved using the ε -constraint approach [Chankong and Haimes 2008], where the resilience objective is converted into a constraint and assigned with the values between 0 and 1 such as $\varepsilon \in [0,1]$ as in Eq. (3313).

$$\sum_{k \in K} \mu^k \sum_{t=1}^{\tau} \left(\frac{t \left[\sum_{i \in N_d^k} (Q_i^k V_i^k P_i^k) - \sum_{i \in N_d^k} (s_{it}^k V_i^k P_i^k) \right] - (t-1) \left[\sum_{i \in N_d^k} (Q_i^k V_i^k P_i^k) - \sum_{i \in N_d^k} (s_{i(t-1)}^k V_i^k P_i^k) \right]}{\sum_{i \in N_d^k} (\tau Q_i^k V_i^k P_i^k)} \right) \leq \varepsilon \quad (47)$$

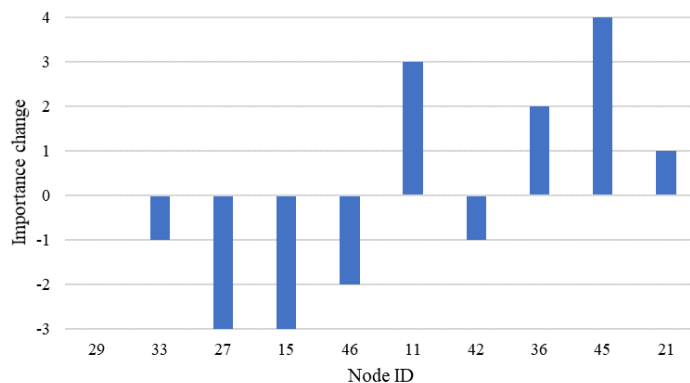
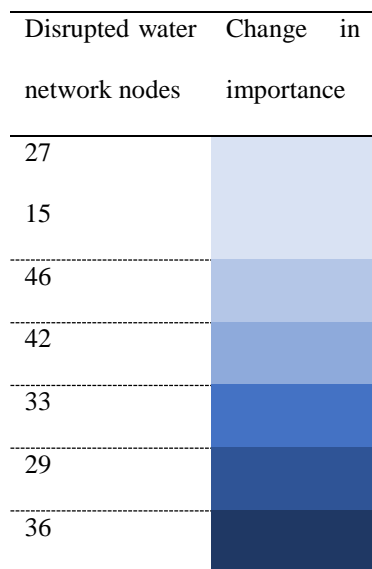
4.1.2. Disruption and Restoration

The disruption scenarios each representing a different earthquake magnitude ($M_w = 6$, $M_w = 7$, $M_w = 8$, $M_w = 9$) are implemented. The highest earthquake magnitude ($M_w = 9$) results in a total of 43 disrupted components, 19 of which are demand nodes. For the restoration process, two work crews are assigned to each infrastructure network. A time horizon of 28 periods is considered to complete the recovery for all four earthquake scenarios.

Among the four disruption scenarios, the two with higher earthquake magnitudes ($M_w = 8, M_w = 9$) represent significant differences in the optimal restoration schedules between the inclusion and exclusion of social vulnerability and population density measures. The other two earthquake scenarios with lower magnitudes ($M_w = 6, M_w = 7$) contain few disrupted components and a low amount of unmet demand, therefore the inclusion of social and population measures does not result in a significant difference in restoration scheduling

As such, the focus of the analysis on the $M_w = 8$ and $M_w = 9$ disruption scenarios, and it represents the effect of including social vulnerability and population density measures by the change in the restoration order of disrupted nodes. Figure 10 through Figure 12 illustrate the change in order for $M_w = 8$ scenarios for water, gas, and power networks, respectively, and likewise Figure 13 through Figure 15 for $M_w = 9$ scenarios. The change in the importance of components is measured as follows: (i) the optimal restoration schedules are obtained for two separate cases: including and excluding social vulnerability and population, (ii) the restoration

order of the disrupted components is listed for each network, and (iii) the difference in orders for each component is calculated with and without social vulnerability and population measures. If this difference is zero, then this means that the restoration order of this component is the same in both cases, suggesting the importance of this component did not change between the two approaches. However, a positive difference suggests that the restoration of the component is scheduled earlier when social vulnerability and population density of its service area is taken into account, suggesting that such measures make the component a priority. Lighter shades represent components with less importance when the social vulnerability and population measures are considered. Note that the darkest shaded components might not necessarily be the most important component in the restoration scheduling, but it is the component that has the biggest change in its restoration order, thus the biggest change in its importance when additional measures are included in the optimization model. While only demand nodes are considered for weighting with social and population measures, naturally supply and transshipment nodes are important to meeting demand (at those weighted demand nodes).



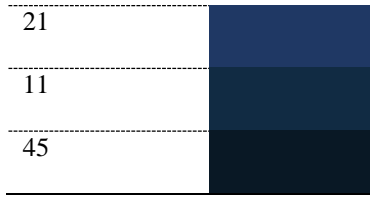


Figure 10. The change in the importance of the disrupted supply, transshipment, and demand nodes in the water network when the community perspective is considered with the earthquake magnitude $M_w = 8$, where lighter blue represents higher negative change and darker blue represents higher positive change.

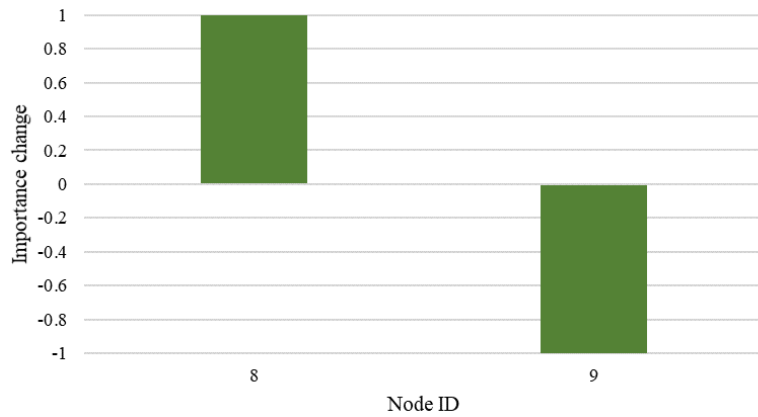
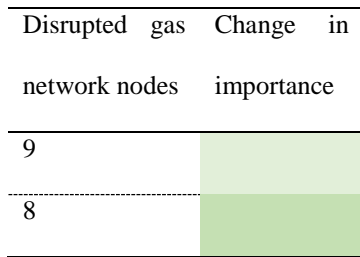


Figure 11. The change in the importance of the disrupted supply, transshipment, and demand nodes in the gas network when the community perspective is considered with the earthquake magnitude $M_w = 8$, where lighter green represents higher negative change and darker green represents higher positive change.

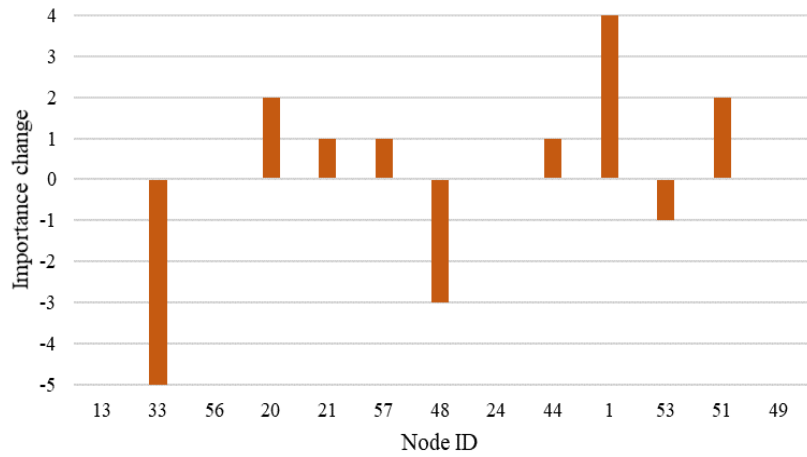
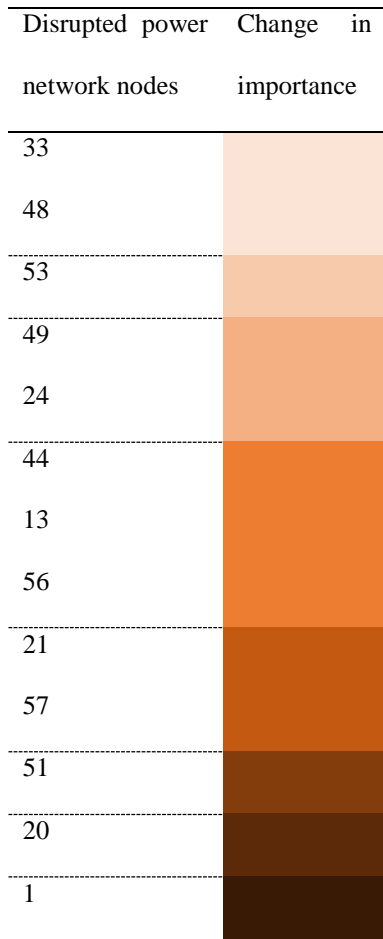


Figure 12. The change in the importance of the disrupted supply, transshipment, and demand nodes in the power network when the community perspective is considered with the earthquake magnitude $M_w = 8$, where lighter orange represents higher negative change and darker orange represents higher positive change.

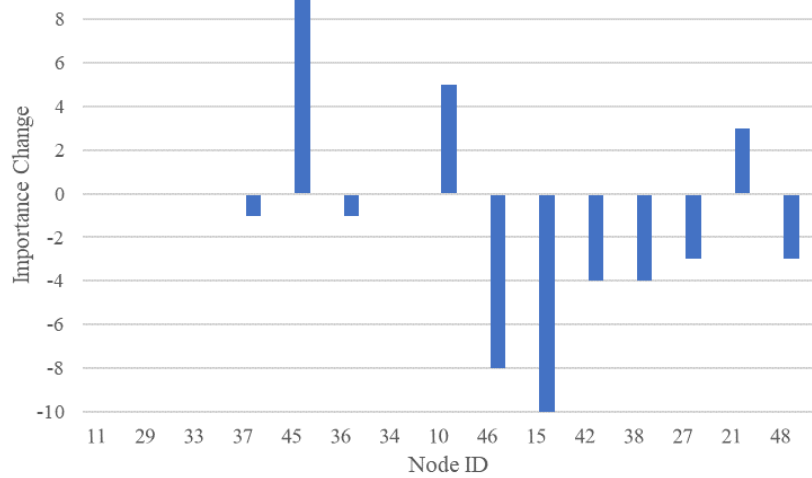
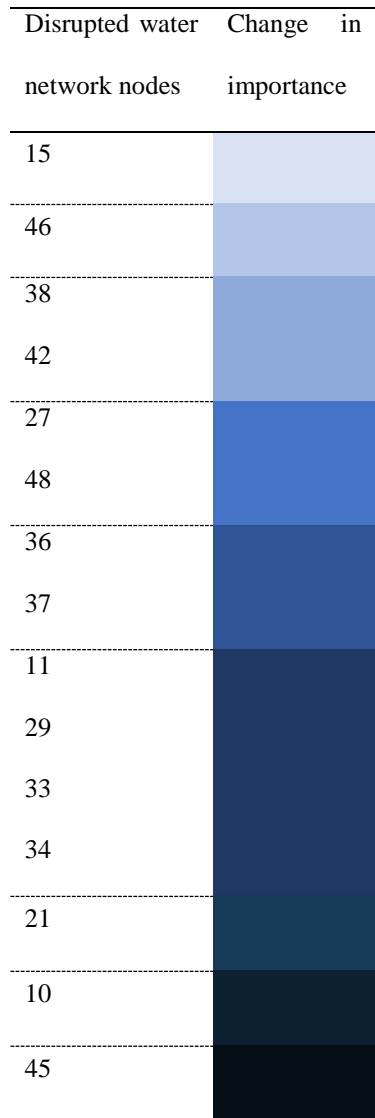


Figure 13. The change in the importance of the disrupted supply, transshipment, and demand nodes in the water network when the community perspective is considered with the earthquake magnitude $M_w = 9$, where lighter blue represents higher negative change and darker blue represents higher positive change.

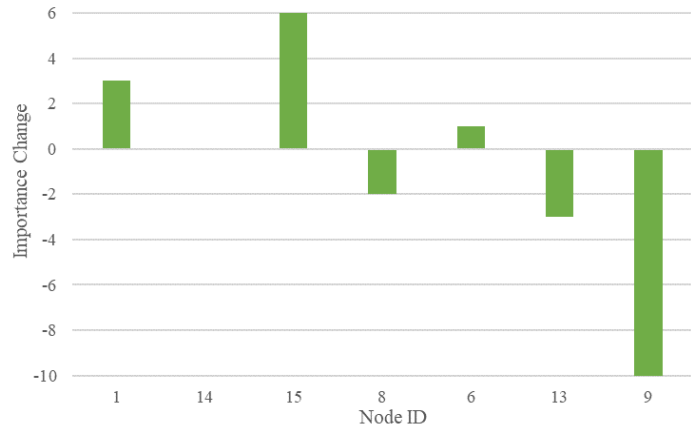
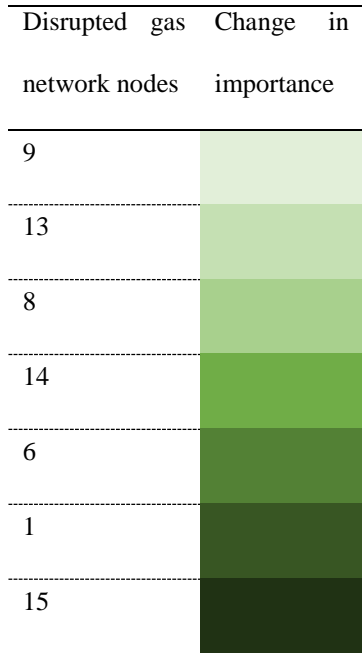
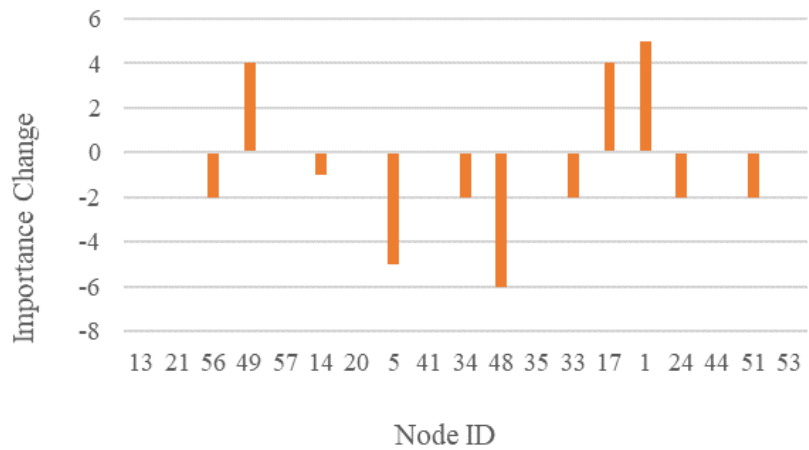
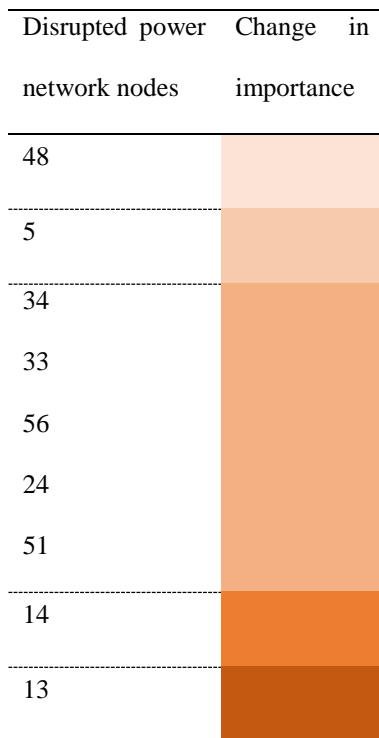


Figure 14. The change in the importance of the disrupted supply, transshipment, and demand nodes in the gas network when the community perspective is considered with the earthquake magnitude $M_w = 9$, where lighter green represents higher negative change and darker green represents higher positive change.



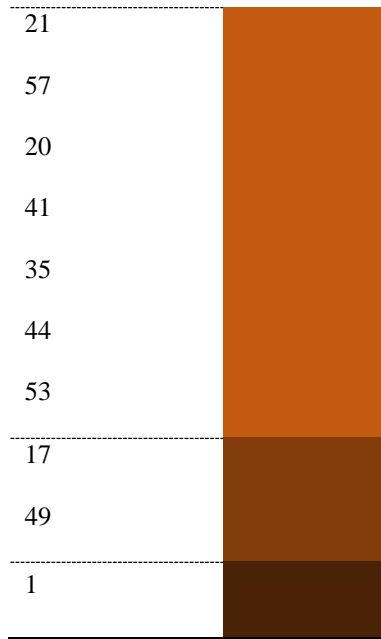
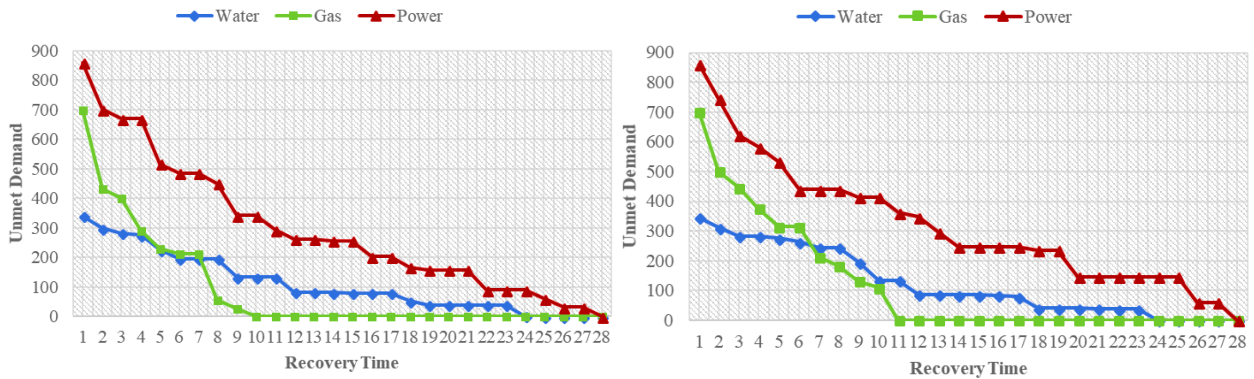


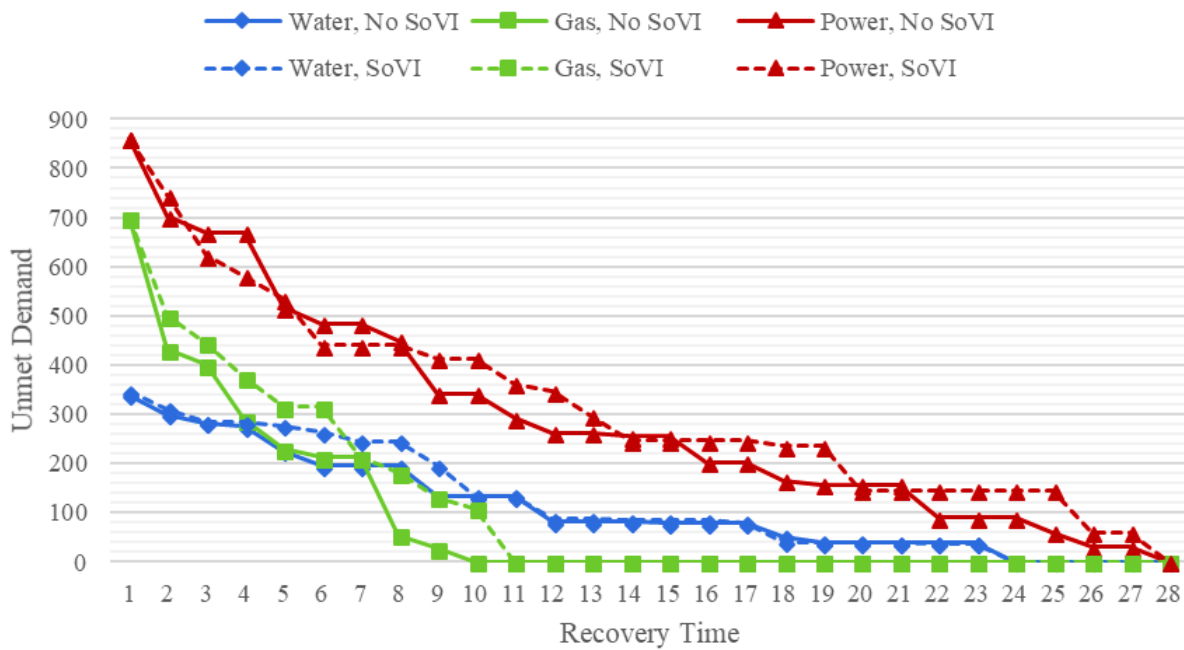
Figure 15. The change in the importance of the disrupted supply, transshipment, and demand nodes in the power network when the community perspective is considered with the earthquake magnitude $M_w = 9$, where lighter orange represents higher negative change and darker orange represents higher positive change.

The trajectory of the system performance over time is illustrated by the unmet demand change in Figure 16 to compare the effect on restoration when social vulnerability and population density are accounted for in the analysis. As it can be seen from these three plots, the unmet demand over time varies for each network when community resilience measures are taken into account.



(a)

(b)



(c)

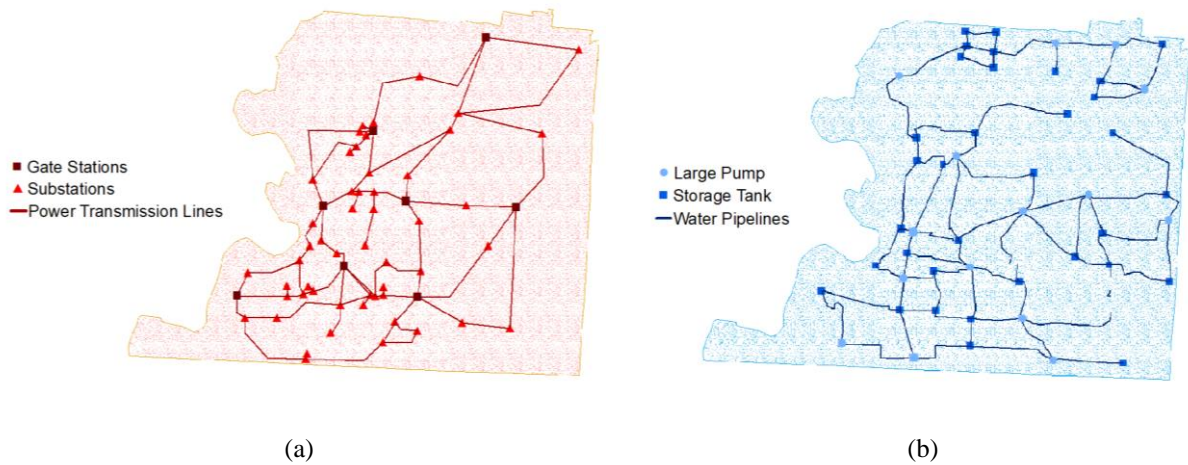
Figure 16. Illustration of unmet demand over the recovery time (a) without SoVI, (b) with SoVI, and (c) comparison on the same plot where dashed lines represent the consideration and solid lines represent the inconsideration of social vulnerability and population density.

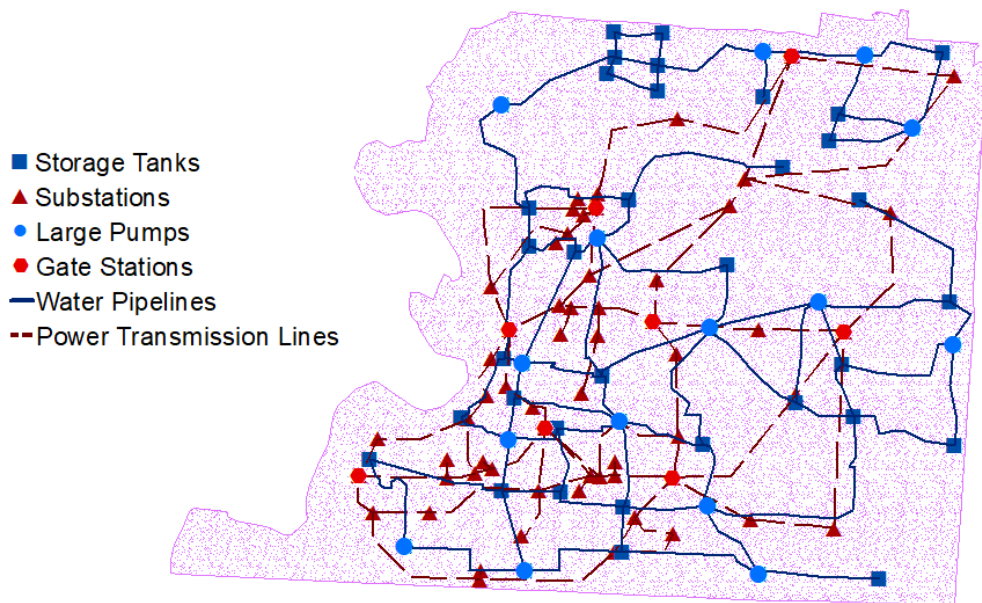
Finally, to validate the differences between the optimal restoration schedules (without SoVI, with SoVI) for the critical infrastructure networks in Shelby County, and to highlight the contribution of the proposed study, we formulated a model to minimize the sum of differences in the restoration times of each disrupted component between the without SoVI and with SoVI

models. At the end, this study did not find a zero distance result, suggesting that there is not one restoration schedule that is optimal for both models. Therefore, it can be concluded that accounting for social vulnerability in restoration schedule indeed changes the optimal scheduling and assignment solution.

4.2. Resilience-Driven Component Importance Measure

In this part of the research, two physically interdependent infrastructure networks, water distribution and electric power networks, the geographic layout of which is represented in Figure 17, both independently and combined are considered. The two infrastructure networks contain a total of 108 nodes, including 15 demand nodes in the water network and 9 demand nodes in the power network. From both of these interdependent infrastructure networks, there are a total of 288 links and through the restoration process. We assign six work crews separately for each network.





(c)

Figure 17. The geographic layout of power and water distribution systems in Shelby County, TN independently and interdependently, respectively (adapted from González et al. [2016]).

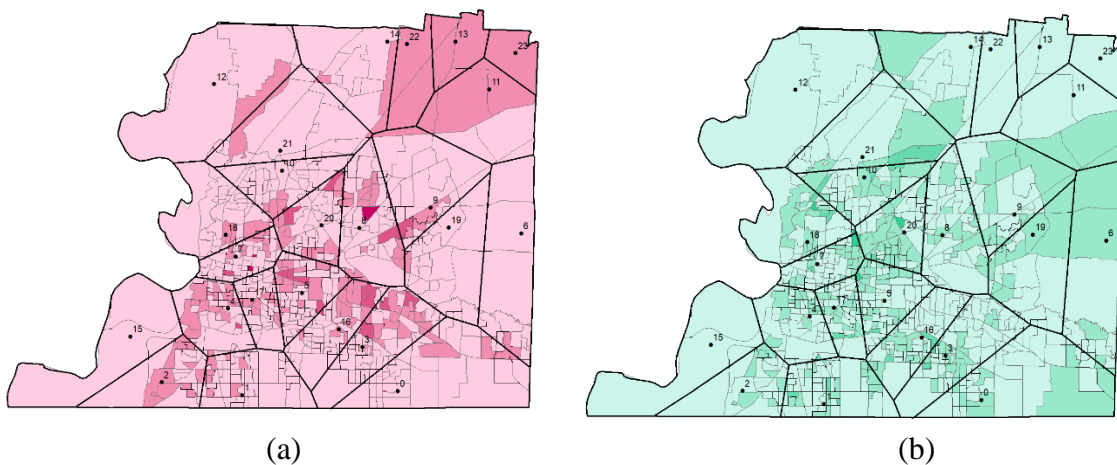
4.2.1. Social Vulnerability Variables

The social vulnerability measures included in the SoVI algorithm [Cutter et al. 2003] were collected for Shelby County, TN. Most of the 11 social vulnerability factors in Table 1 are accounted for with the eight social vulnerability variables listed in Table 4. The provided social vulnerability variables are determined similarly with the community resilience part of the previous study based on correlation analysis [Karakoc et al. 2019].

Table 4. The complete final list of the social vulnerability variables that are utilized in the community-resilience study of Shelby County, TN which are defined by Cutter et al. [2003] as the percentages.

Population over the age of 65	Single-female based households
Population under the age of 5	Households that are in poverty
Population that is Hispanic	

Similarly, with the previous study, the social vulnerability scores, V_{ic}^k , are assigned to the demand nodes at the block group level by utilizing Voronoi diagram approach. The estimated Voronoi coverage areas for each demand node in the two critical infrastructure networks appear as the dark boundaries in Figure 18 and they lay on top of the block groups. The shading of the block groups indicates the strength of social vulnerability index, $SoVI_{ic}^k$, for each of the five variables, which are encoded as “65+,” “5-,” “Hispanic,” “Single-Female,” and “Poverty.” To assign the associated social vulnerability indices to the demand nodes, the average of the indices of the block groups that are located in the Voronoi coverage area is taken and assigned to each demand node. Additionally, we also assign the associated population density values to demand nodes based on the proportional population density of each Voronoi coverage area.



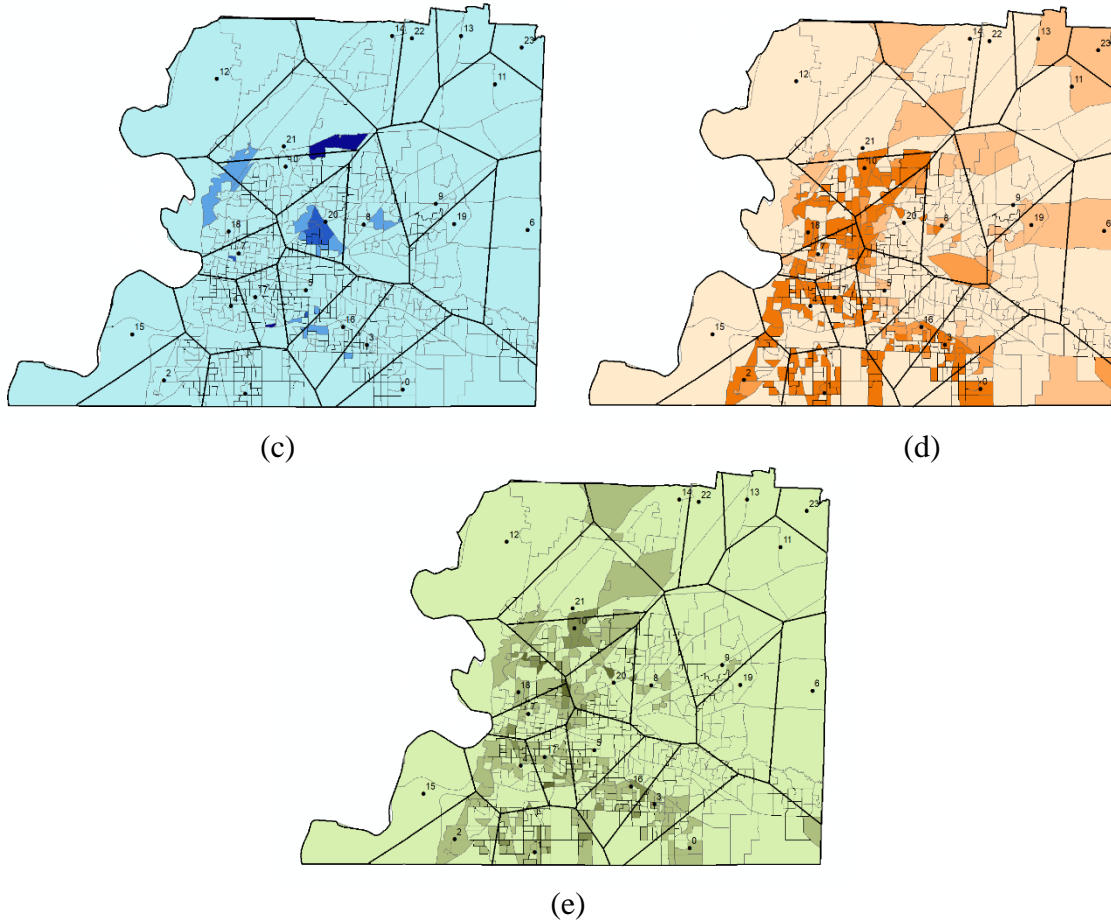


Figure 18. The distribution of social vulnerability scores over the block groups in Shelby County, TN based on the population that is (a) under age five, (b) over age sixty-five, (c) Hispanic, (d) living in poverty, and (e) living in a single-female household whereas with the darker shades, socially more vulnerable region is represented.

For variable $c \in C$, the value of V_{ic}^k is scaled between zero and one, and the social vulnerability scores are grouped in the following four intervals: 0-0.25, 0.25-0.5, 0.5-0.75 and 0.75-1, ranging from the least socially vulnerable to the most socially vulnerable region. The darker the map shading, the higher the social vulnerability is illustrated. As illustrated in Figure 18, some block groups are especially vulnerable with respect to some variables and not with others, suggesting that considering only one variable may not provide a sufficient perspective.

To solve the multi-objective interdependent infrastructure network restoration problem, we utilize the ε -constraint approach [Chankong and Haimes 2008]. Maximizing social equity is kept as the objective of the model, and the resilience maximization objective is converted into a constraint, shown in Eq.(421), as the resilience measure naturally ranges from 0 to 1. Also, minimizing the total cost associated with the restoration process objective is converted into a budget constraint as in Eq. (421), where the budget limit, D , is determined by the decision maker.

$$\sum_{k \in K} \mu^k \sum_{t=1}^{\tau} \left(\frac{t \left[\sum_{i \in N_d^k} (Q_i^k V_i^k P_i^k) - \sum_{i \in N_d^k} (s_{it}^k V_i^k P_i^k) \right] - (t-1) \left[\sum_{i \in N_d^k} (Q_i^k V_i^k P_i^k) - \sum_{i \in N_d^k} (s_{i(t-1)}^k V_i^k P_i^k) \right]}{\sum_{i \in N_d^k} (\tau Q_i^k V_i^k P_i^k)} \right) \leq \varepsilon \quad (48)$$

$$\sum_{k \in K} \left(\sum_{i \in N^k} f n_i^k z_i^k + \sum_{(i,j) \in L^k} f l_{ij}^k y_{ij}^k + \sum_{t \in T} \left[\sum_{(i,j) \in L^k} c_{ij}^k x_{ij}^k + \sum_{i \in N_d^k} p_i^k s_{it}^k V_i^k P_i^k \right] \right) \leq D \quad (49)$$

4.2.3. Disruption Scenarios

In this study, we consider a single disruption scenario of a magnitude 7.0 earthquake, $M_w = 7$. Were a lone earthquake scenario considered, the number of disrupted components would be fixed and the resulting rankings would be specific just to that particular disruption. To capture a more holistic ranking of (most of) the components, we simulate 50 different disruptions with varying disrupted components. In each one of these 50 different cases, the disrupted components are determined according to a previously conducted simulation study by González et al. [2016], and a certain disruption probability is assigned to each component to simulate one of the 50 magnitude 7.0 earthquakes. Across the 50 disruptions, a total of 397 components were disrupted, 109 of which are nodes and the remaining 288 are links. Among these 109 of the nodes, 49 of them belong to the water network and the remaining 60 of them belong to the power network. Among the 288 links, 142 belong to the water network and the remaining 146 from the power network. The number of disrupted components range from 28 to 60 in the individual disruption scenario simulations. In this study, we run the proposed restoration scheduling of interdependent

infrastructure network model for 50 disruption scenarios with varying disrupted components. This step is repeated five times to reflect the optimal restoration scheduling for each of the five social vulnerability variable perspectives. As such, we calculate the ORT for each variable separately, where disrupted components with smaller restoration completion time earn higher priority and receive smaller rank values. As the restoration completion time of the disrupted components increase, their priority decrease and the components are assigned with higher ranking values, thus lower importance levels.

To aggregate the 50 different disruption scenarios, we develop an aggregation index that determines the final rank of each disrupted component. This index is calculated with the following: (i) the disrupted components in each disruption scenario are ranked separately using ORT, (ii) the ranks of each disrupted component are represented with $\frac{i}{g}$, where i refers to the rank of the disrupted component and g refers to the total number of disrupted components in each scenario, such that $g \in [28, 60]$ [Kolesárová et al. 2007], and finally (iii) the $\frac{i}{g}$ values are averaged based on the number of scenarios that each component is disrupted [Muralidharan et al. 2002, Ho et al. 2009]. That is, even though there are a total of 50 disruption scenarios, if a single component is disrupted in only a of these scenarios, we calculate the average based on the h , where $h \leq g$, scenarios such that the randomness of the simulation does not influence a component's ranking. The aggregation index applies simple arithmetic on the ordinal data, however this practice is motivated by the literature [Kolesárová et al. 2007, Muralidharan et al. 2003, Ho et al. 2009].

4.2.4. Integration of Rankings with TOPSIS

Discussed previously, different network components are important from different social vulnerability perspectives. To aggregate these different perspectives into a comprehensive ranking of infrastructure components that affect community resilience, we implement a multi-criteria

decision analysis technique, TOPSIS. Recall that with TOPSIS, the set of alternatives, A , is ranked across multiple criteria, C . With the application of TOPSIS in our study, the alternatives to be ranked consist of the set of 397 disrupted components, and the multiple criteria consist of the set of the five social vulnerability variables. The performance scores of the set of alternatives under each criteria, Y_{ec} , represents the aggregation index of the ranks of the disrupted components whose values range from $[0.017,1]$. The five social vulnerability variables represent “costs” (e.g., values to be minimized) from an MCDA perspective. And since a better ranking is the result of a smaller aggregation index, the positive ideal solution for each variable is its smallest aggregation index.

To find the weights of each social vulnerability variable, ω_c , we utilize the Principle Component Analysis (PCA) technique, a widely used approach to aggregate multiple inputs with the minimum loss of information [Adler and Golany 2000]. The PCA method explains the variance structure of data through linear combinations of variables [Johnson and Wichern 1982], where the dynamics of the information exist along directions with the largest variance [Shlens 2014]. Hence, it is not uncommon to use the “percent variation in a dependent variable explained by an independent variable” to measure the importance of the effect of the independent one on the dependent one [Rosenthal and Rubin 1979]. Similarly, we assume that the amount of variance that is captured by each social vulnerability variable could stand for the importance of that variable relative to the others. More information about the formulation and definition of the PCA approach can be found in Holland [2008].

To ensure that the weight, the largest variance coverage stands for the most important variable, is consistent with the previous steps of our study where a lower ranking value represents more a more important component, we apply the following scaling approach: (i) calculate the inverse of the original weight of each social vulnerability variable found from PCA, (ii) sum these

inverse values, and (iii) scale them with the ratio of each over their sum. As such, the newly calculated weight values are consistent with the ranking of the components based on their importance (i.e., higher weight values suggest less important social vulnerability variable) and have a sum that is equal to 1. The explained scaling approach with the final criteria weights, ω_c'' is formulated in Eq. (50)-(52) where $\sum_{c=1}^m \omega_c'' = 1$, and the calculated final weights of the five social vulnerability variables are listed in Table 5.

$$\omega'_c = \frac{1}{\omega_c}, \quad c = 1, \dots, m \quad (50)$$

$$S = \sum_c \omega'_c, \quad c = 1, \dots, m \quad (51)$$

$$\omega_c'' = \frac{\omega'_c}{S}, \quad c = 1, \dots, m \quad (52)$$

Table 5. The representation of the weights of the social vulnerability variables that are determined by PCA method and utilized in TOPSIS algorithm.

Population that is over the age 65	0.22
Population that is under the age 5	0.22
Population that is Hispanic	0.23
Single-female parent based households	0.17
Households living under the poverty line	0.16

Table 5 suggests that the weights that are assigned to each social vulnerability variable are relatively similar. Despite the PCA weights of social vulnerability variables being close to each other, a systematic and data-driven approach was used, allowing for a better informed decision making process relative to random (or strictly equal) weights.

4.2.5. Critical Components of Shelby County, TN

The components that make up the top 10 rankings for each social vulnerability variable are depicted in Figure 20 and Figure 19 for the water and power networks, respectively. For the power network, we see some variability in ranking among the components for the different social vulnerability variables (e.g., most of the top five components have very similar ranks for each variable), perhaps suggesting that social vulnerability does have a little impact restoration order for that network. The water network, however, demonstrates more variability: there is a wider variety of components and different types of components (i.e., both links and nodes) in the top ten. In both networks, the most important component according to ORT stands out across social vulnerability variables. Note that of the 32 components that appear across the top 10 rankings of the two networks, only two of them are links, and as the component rankings are aggregated based on a multi-criteria decision analysis technique, the top ten components result as all nodes. The obtained results suggest that nodes are overwhelmingly more critical from ORT and social vulnerability perspectives.

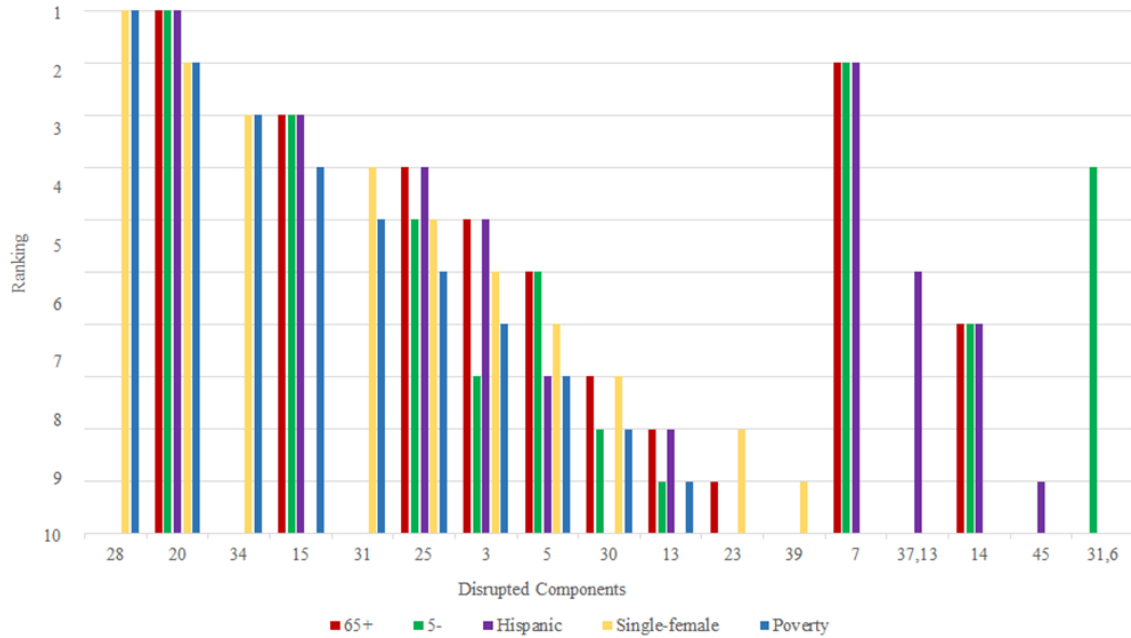


Figure 20. The ranking of the subset of the water network components (both nodes and links are listed) are represented independently based on each social vulnerability variable.

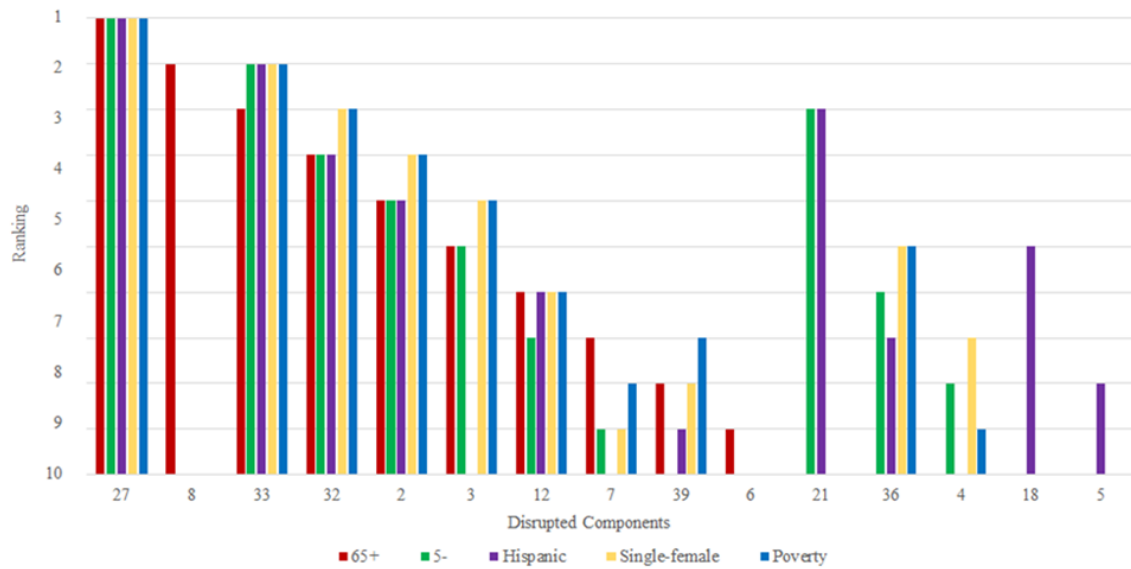


Figure 19. The ranking of the subset of power network components (both nodes and links are listed) are represented independently based on each social vulnerability variable.

Integrating the rankings with TOPSIS results in Table 6. The integrated rankings are quite similar to Figure 20 and Figure 19 due in part to the lack of variability in the individual rankings of many of the social vulnerability variables and due to the similarity of variable weights from Table 5. As it can be seen, the water network has relatively higher variance than power network in terms of the ranking of the critical components under different social vulnerability measures. This could be due to the difference in size and connectivity of the two networks.

Table 6. A subset of the critical components (both nodes and links are considered) in the water and power network based on all the available social vulnerability measures together.

Rank by ORT	Water network components	Power network components
1	Node 20	Node 27
2	Node 25	Node 33
3	Node 15	Node 32
4	Node 3	Node 2
5	Node 5	Node 12
6	Node 45	Node 7
7	Node 8	Node 3
8	Node 4	Node 19
9	Node 18	Node 6
10	Node 6	Node 39

Chapter 5: Concluding Remarks

Due to the globalization of networks and the developments in the infrastructure technology, interdependencies among critical infrastructure networks are being formed incrementally. Such enhanced interdependencies result in more complex and vulnerable systems, where it becomes more challenging for the decision makers to plan their recovery after a disruptive event. Additionally, the dependency of the surrounding communities over these networks and their social vulnerabilities increase the possible impacts of the disruptive events, by hardening the problem of recovery planning both for the system and the society.

In this research, the interdependent infrastructure network restoration problem is studied and an optimization model from the community resilience perspective is proposed. The proposed model plans the restoration schedule for each network by (i) prioritizing the disrupted components, and (ii) assigning them to available work crews for specific time periods according to their relative importance on the overall system resilience. The aim of prioritizing the disrupted components and enhancing the resilience of physically interdependent infrastructure networks consider the community resilience perspective through the restoration scheduling process as each demand node is assigned with the (i) social vulnerability score and the (ii) population density of the residential area they represent.

Furthermore, understanding the relationship between the certain socio-economic characteristics and the different components of the networks is the first step to identifying component criticality. The interdependent infrastructure networks restoration problem and the identification of critical components in the system is studied where a multi-objective optimization model from the community resilience perspective that (i) maximizes the overall system resilience for a given restoration horizon, (ii) minimizes the total cost associated with the restoration process,

and (iii) maximizes the social equity through the scheduling of restoration process is proposed. The proposed model plans for the restoration schedule of the interdependent infrastructure networks by prioritizing the disrupted components that serve socially less advantageous communities based on their social demographics and resilience levels. This approach ensures that the restoration process of the interdependent infrastructure networks is motivated by social equity and community resilience perspectives.

Additionally, the proposed model considers various social vulnerability measures where each demand node in the critical networks are assigned with (i) a specific social vulnerability score for each social vulnerability variable separately, and (ii) population density of its related service area in order to represent the service expectations from community perspective. In this study, the proposed approach allows us to determine the critical infrastructure components according to the planned restoration schedule with the utilization of resilience-based component importance measure, ORT. The critical components are ranked according to their restoration time due based on multiple social vulnerability measures. For the results of this study, it is observed that through the restoration of two critical infrastructures in Shelby County, the majority of the earlier periods of the restoration horizon are reserved for the nodes of the networks as they are responsible for more drastic increase in the system resilience both for the case of considering each social vulnerability measure independently and together where they are aggregated by TOPSIS algorithm. Hence, through the pre-disruption preparedness planning and the post-disruption recovery process, the decision-makers could schedule the restoration of the disrupted nodes prior to the disrupted links. For the schedule of the nodes among each other, in that case, the decision makers can base their implementations on the relative importance of the social vulnerability measures.

The social vulnerability scores are calculated with a reduced approach of Social Vulnerability Index [Cutter et al. 2003], in order to account for the major social dimensions in the community, -such as age, income level, and race attainments. Also, population densities are calculated to measure the human occupancy in the surrounding of the network components. These community resilience measures are added to a mixed-integer multi-objective resilience-driven restoration model, which maximizes the cumulative community resilience of the interdependent infrastructure networks over time while considering the total cost associated with the restoration process.

As for the results of the study, it is observed that accounting for the community resilience measures in the restoration planning of interdependent infrastructure networks definitely affects the scheduling of the disrupted components since there exists no such restoration schedule that is optimal for both including and excluding community resilience measures. As expected, disrupted components that represent socially more vulnerable and denser regions are prioritized in the restoration process. Thus, the components with higher priority correspond to not only the ones with large unmet demands in their service area, but also to the ones that are responsible for the supply and transshipment of commodities to socially more vulnerable communities.

For future work, the model could be extended to consider partial disruptions, such that the system can operate with reduced capacities. Moreover, partial physical dependencies could be included in the proposed model, where a component could be partially functional, if the components upon which it depends are partially operational. Additionally, the proposed community resilience-based prioritization and scheduling process could be combined with geographical hazard metrics to account for spatial risks associated with the specific location of the network components. Furthermore, additional resilience-based component importance measures

could be considered to determine and rank the critical components of the interdependent infrastructure networks. Moreover, more critical infrastructure networks that are interdependent in nature could be included in the study with various types of interdependencies, and the community-resilience perspective could be extended to incorporate with different types of interdependencies to provide a more comprehensive study of interdependent infrastructure network restoration and component importance measures problem.

References

- Adler, N. and B. Golany. 2000. The use of data envelopment analysis in determining choice of airline networks under deregulation. *European Journal of Operations Research*.
- Aksu, D.T. and L. Ozdamar. 2014. A Mathematical Model for Post-Disaster Road Restoration: Enabling Accessibility and Evacuation. *Transportation Research Part E: Logistics and Transportation*, **61**(1): 56-67.
- Almoghathawi, Y., K. Barker, and L. Albert. 2019. Resilience-Driven Restoration Model for Interdependent Infrastructure Networks. *Reliability Engineering and System Safety*, **185**: 12-23.
- Almoghathawi, Y., K. Barker, and L. Albert. 2017. Component Importance Measures for Interdependent Infrastructure Network Resilience. Manuscript submitted for publication.
- Arnette, A.N. and C.W. Zobel. 2019. A Risk-Based Approach to Improving Disaster Relief Asset Pre-Positioning. *Production and Operations Management*, **28**(2): 457-478.
- Auf der Heide, E. and J. Scanlon. 2007. Health and medical preparedness and response. *Emergency management: Principles and practice for local government*, 183-206.
- Aven, T. 2010. On Some Recent Definitions and Analysis Frameworks for Risk, Vulnerability, and Resilience. *Risk Analysis: An International Journal*, **31**(4): 515-522.
- Ayyub, B. M. and P. E. F. Asce. 2011. Vulnerability, uncertainty, and risk: analysis, modelling and management. Proceedings of the ICVRAM 2011.
- Baidya, P.M. and W. Sun. 2017. Effective Restoration Strategies of Interdependent Power System and Communication Network. *The Journal of Engineering*, **1**(1).
- Barabasi, A.L. and R. Albert. 1999. Emergence of Scaling in Random Networks. *Science*, **286**(5439): 509-512.
- Barker, K., D. B. Karakoc and Y. Almoghathawi. 2018. Interdependent Infrastructure Network Restoration Problem from a Community-Resilience Perspective. *Proceedings of the European Safety and Reliability Conference*, Trondheim, NOR.
- Barker, K., J.H. Lambert, C.W. Zobel, A.H. Tapia, J.E. Ramirez-Marquez, L.A. McLay, C.D. Nicholson, and C. Caragea. 2017. Defining Resilience Analytics for Interdependent Cyber Physical-Social Networks. *Sustainable and Resilient Infrastructure*, **2**(2): 59-67.
- Barker, K., J.E. Ramirez-Marquez, and C.M. Rocco. 2013. Resilience-based Network Component Importance Measures. *Reliability Engineering and System Safety*, **117**: 89-97.
- Blaikie, P., T. Cannon, I. Davis and B. Wisner. 1994. At Risk: Natural Hazards, People's Vulnerability and Disasters. Routledge.

Buldyrev, S.V., R. Parshani, G. Paul, H.E. Stanley, and S. Havlin. 2010. Catastrophic Cascade of Failures in Interdependent Networks. *Nature*, **464**(7291): 1025-1028.

Cai, X. 2008. Water stress, water transfer and social equity in Northern China Implications for policy reforms. *Journal of Environmental Management*, **87**(1): 14-25.

Cao, W., M. Çelik, O. Ergun, J. Swann, and N. Viljoen. 2016. Challenges in service network expansion: An application in donated breastmilk banking in South Africa. *Socio-Economic Planning Sciences*, **53**: 33-48.

Castells, M. 1996. *The Rise of the Network Society. The Information Age: Economy, Society, and Culture Volume I (Information Age Series)*. London: Blackwell.

Cavdaroglu, B., E. Hammel, J.E. Mitchell, T.C. Sharkey, and W.A. Wallace. 2013. Integrating restoration and scheduling decisions for disrupted interdependent infrastructure systems. *Annals of Operations Research*, **203**(1): 279-294.

Chankong, V. and Y. Y. Haimes. 2008. *Multiobjective Decision Making: Theory and Methodology*. Dover Books on Engineering. Courier Dover Publications.

Cimellaro, G., A. Reinhorn, and M. Bruneau. 2010. Seismic Resilience of a Hospital System. *Structure and Infrastructure Engineering*, **6**(1): 127-144.

Coffrin C., P. Van Hentenryck, and R. Bent. 2012. Last-Mile Restoration for Multiple Interdependent Infrastructures. In: *Proceedings of the 26th AAAI conference on Artificial Intelligence*, Toronto, Canada, July 22–26, **12**: 455-463.

Cutter, S. L., C. T. Emrich, D. P. Morath, and C. M. Dunning. 2013. Integrating social vulnerability into federal flood risk management planning. *Journal of Flood Risk Management*, **6**(4): 332-344.

Cutter, S. L., L. Barnes, M. Berry, C. Burton, E. Evans, E. Tate and J. Webb. 2008. A place-based model for understanding community resilience to natural disasters. *Global Environmental Change*, **18**(4): 598-606.

Cutter, S.L., B.J. Boruff & W.L. Shirley. 2003. Social Vulnerability to Environmental Hazards. *Social Science Quarterly*, **84**(1): 242-261.

Davis, L. B., F. Samanlioglu, X. Qu, and S. Root. 2013. Inventory planning and coordination in disaster relief efforts. *International Journal of Production Economics*, **141**(2): 561-573.

Department of Homeland Security. 2013. National Preparedness Report.

Eusgeld, I., C. Nan, and S. Dietz. 2011. “System-of-systems” approach for interdependent critical infrastructures. *Reliability Engineering and System Safety*, **96**(6): 679-686.

- Evans, J.M., D. Hardy, M. Hauer. 2014. Assessing Social Vulnerability using “SoVI-Lite:” A Demonstration Study at Glynn County, GA.
- Fang, Y.P., N. Pedroni, and E. Zio. 2016. Resilience-Based Component Importance Measures for Critical Infrastructure Network Systems. *IEEE Transactions on Reliability*, **65**(2): 502-512.
- Gong, J., E.E. Lee, J.E. Mitchell, and W.A. Wallace. 2009. Logic-based multiobjective optimization for restoration planning. In *Optimization and Logistics Challenges in the Enterprise* (pp. 305-324). Springer US.
- González, A.D., A. Chapman, L. Dueñas-Osorio, M. Mesbahi, and R. D’Souza. 2017. Efficient Restoration Strategies using the Recovery Operator. *Computer-Aided Civil and Infrastructure Engineering*, **32**(12): 991-1006.
- González, A.D., L. Dueñas-Osorio, M. Sánchez-Silva, and A.L. Medaglia. 2016. The Interdependent Network Design Problem for Optimal Infrastructure System Restoration. *Computer-Aided Civil and Infrastructure Engineering*, **31**(5): 334-350.
- Graham, S. 2000. Constructing premium network spaces: reflections on infrastructure networks and contemporary urban development. *International Journal of Urban and Regional Research*, **24**(1): 183-200.
- Graham, S. 2000. Introduction: Cities and Infrastructure. *International Journal of Urban and Regional Research*, **24**(1): 114-119.
- Gralla, E., J. Goentzel, and C. Fine. 2014. Assessing trade-offs among multiple objectives for humanitarian aid delivery using expert preferences. *Production and Operations Management*, **23**(6): 978-989.
- Haimes, Y. Y. 2009. On the Definition of Resilience in Systems. *Risk Analysis: An International Journal*, **29**(4): 498-501.
- Henry, D., and J.E. Ramirez-Marquez. 2012. Generic Metrics and Quantitative Approaches for System Resilience as a Function of Time. *Reliability Engineering and System Safety*, **99**(1): 114-122.
- Ho, William, Xiaowei Xu, and Prasanta K. Dey. 2010. Multi-criteria decision making approaches for supplier evaluation and selection: A literature review. *European Journal of operational research*, **202**(1): 16-24.
- Holden, R, D.V. Val, R. Burkhard, and S. Nodwell. 2013. A Network Flow Model for Interdependent Infrastructures at The Local Scale. *Safety Science*, **53**(1): 51-60.
- Holland, S. M. 2008. Principal components analysis (PCA). Department of Geology, University of Georgia, Athens, GA, 30602-2501.

- Holmgren, A.J. 2006. Using Graph Models to Analyze the Vulnerability of Electric Power Networks. *Risk Analysis: An International Journal*, **26**(4): 955-969.
- Hosseini, S., K. Barker and J. E. Ramirez-Marquez. 2016. A review of definitions and measures of system resilience. *Reliability Engineering and System Safety*, **145**: 47-61.
- Huang, M., K. Smilowitz, and B. Balcik. 2012. Models for relief routing: Equity, efficiency and efficacy. *Transportation Research Part E*, **48**(1): 2-18.
- Hwang, Ching-Lai, and Kwangsun Yoon. 1981. Methods for multiple attribute decision making. *Multiple attribute decision making*. Springer, Berlin, Heidelberg, 58-191.
- Johnson, Richard A., and D. W. Wichern. 1982. Applied multivariate statistics. *Englewood Cliffs*, NJ: Prentice Hall.
- Joseph, K.T., K. Rice, and C. Li. 2016. Integrating Equity in a Public Health Funding Strategy. *Journal of Public Health Management and Practice*, **22**(1): 68-76.
- Jönsson, H., J. Johansson and H. Johansson. 2008. Identifying Critical Components in Technical Infrastructure Networks. *Journal of Risk and Reliability*, **222**(2): 235-243.
- Kamamura, S., D. Shimazaki, K. Genda, K. Sasayama, and Y. Uematsu. 2015. Disaster Recovery for Transport Network through Multiple Restoration Stages. *IEICE Transactions on Communications*, **98**(1): 171-179.
- Karakoc, D. B., Y. Almoghathawi, K. Barker, A. D. González and S. Mohebbi. 2019. Community Resilience-Driven Restoration Model for Interdependent Infrastructure Networks, Manuscript submitted for publication to *International Journal of Disaster Risk Reduction*.
- Kolesárová, Anna, Gaspar Mayor, and Radko Mesiar. 2007. Weighted ordinal means. *Information Sciences*, **177**(18): 3822-3830.
- LaRocca, J. Johansson, H. Hassel and S. Guikema. 2014. Topological Performance Measures as Surrogates for Physical Flow Models for Risk and Vulnerability Analysis for Electric Power Systems. *Risk Analysis: An International Journal*, **35**(4): 608-623.
- Lee, E.E., J.E. Mitchell, and W.A. Wallace. 2007. Restoration of services in interdependent infrastructure systems: A network flows approach. *Systems, Man, and Cybernetics, Part C: Applications and Reviews, IEEE Transactions on*, **37**(6): 1303-1317.
- Li, Y. and B.J. Lence. 2007. Estimating Resilience of Water Resources Systems. *Water Resources Research*, **43**(7): W07422.
- Little, R.G. 2002. Controlling Cascading Failure: Understanding the Vulnerabilities of Interconnected Infrastructures. *Journal of Urban Technology*, **9**(1): 109-123.

Lootsma, F. A. 1999. Multi-criteria decision analysis via ratio and difference judgement, *Kluwer Academic Publishers*, **29**, Norwell, MA.

Manaugh, K., M. G. Badami, and A. M. El-Geneidy. 2015. Integrating social equity into urban transportation planning: A critical evaluation of equity objectives and measures in transportation plans in North America. *Transport Policy*, **37**: 167-176.

Manaugh, K., and A. El-Geneidy. 2012. Who benefits from new transportation infrastructure? Using accessibility measures to evaluate social equity in public transport provision. *Chapters*, 211-227.

Matisziw, T.C., A.T. Murray, and T.H. Grubestic. 2010. Strategic Network Restoration. *Networks and Spatial Economics*, **10**(3): 345-361.

McAllister, T.P. 2012. Community Resilience of the Built Environment. National Institute of Standards and Technology.

Mileti, D. 1999. Disasters by Design: A Reassessment of Natural Hazards in the United States. *Natural Hazards and Disasters: Reducing Loss and Building Sustainability in a Hazardous World: A Series*. Joseph Henry Press.

Morrow, B. H. 2002. Identifying and Mapping Community Vulnerability. *Disaster*, **23**(1): 1-18.

Muralidharan, C., N. Anantharaman, and S. G. Deshmukh. 2002. A multi-criteria group decision making model for supplier rating. *Journal of supply chain management*, **38**(3): 22-33.

Nagurney, A. and Q. Qiang. 2009. *Fragile Networks: Identifying Vulnerabilities and Synergies in an Uncertain World*. John Wiley & Sons.

National Academies of Science. 2012. *Disaster Resilience: A National Imperative*.

National Research Council. 2006. *Facing Hazards and Disasters: Understanding Human Dimensions*. National Academies Press.

Newman, M. E. J., P. Holme and E. A. Leicht. 2006. Vertex similarity in networks. *Physical Review E*, **73**(2): 026120.

Nicholson, C. D., K. Barker and J. E. Ramirez-Marquez. 2016. Flow-based vulnerability measures for network component importance: Experimentation with preparedness planning. *Reliability Engineering and System Safety*, **145**: 62-73.

Norris, F. H., S. P. Stevens, B. Pfefferbaum, K. F. Wyche and R. L. Pfefferbaum. 2007. Community Resilience as a Metaphor, Theory, Set of Capacities, and Strategy for Disaster Readiness. *American Journal of Community Psychology*, **41**(1-2): 127-150.

Noyan, N., B. Balcik, and S. Atakan. 2015. A stochastic optimization model for designing last mile relief networks. *Transportation Science*, **50**(3): 1092-1113.

Nurre, S.G., B. Cavdaroglu, J.E. Mitchell, and T.C. Sharkey. 2012. Restoring infrastructure systems: an integrated network design and scheduling (INDS) problem. *European Journal of Operational Research*, **223**(3): 794-806.

Obama, B.H. 2013. Critical Infrastructure Security and Resilience. The White House, Washington.

Ogryczak, W., H. Luss, M. Pióro, D. Nace, and A. Tomaszewski. 2014. Fair optimization and networks: A survey. *Journal of Applied Mathematics*, **2014**: 612018.

Okabe, A., T. Satoh, T. Furuta, A. Suzuki, and K. Okano. 2008. Generalized network Voronoi diagrams: Concepts, computational methods, and applications. *International Journal of Geographical Information Science*, **22**(9): 965-994.

Ouyang, M. 2014. Review on modeling and simulation of interdependent critical infrastructure systems. *Reliability engineering & System safety*, **121**: 43-60.

Resilience Alliance. 2009. Adaptive Capacity.

Rinaldi, S.M., J.P. Peerenboom, and T.K. Kelly. 2001. Identifying, Understanding and Analyzing Critical Infrastructure Interdependencies. *IEEE Control Systems Magazine*, **21**(6): 11-25.

Rocco, C. M., J. E. Ramirez-Marquez, D. E. Salazar and I. Hernandez. 2010. Implementation of multi-objective optimization for vulnerability analysis of complex networks. *Proceedings of the Institution of Mechanical Engineers, Part O: Journal of Risk and Reliability*, **224**(2): 87-95.

Rose, A. 2007. Economic Resilience to Natural and Man-Made Disasters: Multidisciplinary Origins and Contextual Dimensions. *Environmental Hazards*, **7**(4): 383-398.

Rosenkrantz, D.J., S. Goel, S.S. Ravi, and J. Gangolly. 2009. Resilience Metrics for Service-oriented Networks: A Service Allocation Approach. *IEEE Transactions on Services Computing*, **2**(3): 183-196.

Rosenthal, Robert, and Donald B. Rubin. 1979. A note on percent variance explained as a measure of the importance of effects. *Journal of Applied Social Psychology*, **9**(5): 395-396.

Rotmans, J., W. E. Walker, P. Harremoës, J. P. van der Sluijs, M. B. A. van Asselt, P. Janssen and M. P. K. von Krauss. 2003. Defining uncertainty: a conceptual basis for uncertainty management in model-based decision support. *Integrated assessment*, **4**(1): 5-17.

Sharkey, T.C., B. Cavdaroglu, H. Nguyen, J. Holman, J.E. Mitchell, and W.A. Wallace. 2015. Interdependent Network Restoration: On the Value of Information-Sharing. *European Journal of Operational Research*, **244**(1): 309-321.

Shlens, Jonathon. 2014. A tutorial on principal component analysis. *arXiv preprint arXiv:1404.1100*

Smith, A.M., A.D. González, L. Dueñas-Osorio, and R.M. D'Souza. 2017. Interdependent Network Recovery Games. *Risk Analysis (In press)*

The Infrastructure Security Partnership. 2011. Regional Disaster Resilience Guide for Developing an Action Plan. Technical report, American Society of Civil Engineers.

The Report of the President's Commission on Critical Infrastructure Protection. 1997. Critical Foundation: Protecting America's Infrastructure. USA.

Thomopoulos, N., S. Grant-Muller, and M.R. Tight. 2009. Incorporating equity considerations in transport infrastructure evaluation: Current practice and a proposed methodology. *Evaluation and Program Planning*, **32**(4): 351-359.

Tierney, K. 2009. Disaster response: Research findings and their implications for resilience measures. Oak Ridge, TN: CARRI Research Report, **6**.

Tootaghaj, D.Z., N. Bartolini, H. Khamfroush, and T. La Porta. 2017. Controlling Cascading Failures in Interdependent Networks under Incomplete Knowledge. In: *Proceedings of the IEEE 36th Symposium on Reliable Distributed Systems, 2017*, Hong Kong, September 26-29, 54-63.

US Census Bureau. 2010. Geographic Terms and Concepts.

Vugrin, E.D., M.A. Turnquist, and N.J. Brown. 2014. Optimal recovery sequencing for enhanced resilience and service restoration in transportation networks. *International Journal of Critical Infrastructures*, **10**(3-4): 218-246.

Wallace, W.A., D.M. Mendonca, E.E. Lee, J.E. Mitchell, J.H. Chow Wallace, and J.L. Monday. 2003. Managing disruptions to critical interdependent infrastructures in the context of the 2001 World Trade Center attack. In *Beyond September 11th: An Account of Post-Disaster Research*, special publication #39, (pp. 165-198), Natural Hazards Research and Applications Information Center, University of Colorado.

Wang, S., L. Hong, M. Ouyang, J. Zhang, and X. Chen. 2013. Vulnerability Analysis of Interdependent Infrastructure Systems Under Edge Attack Strategies. *Safety science*, **51**(1): 328-337.

White House. 2013. Critical Infrastructure Security and Resilience.

Xu, N., S.D. Guikema, R. Davidson, L. Nozick, Z. Cagnan, and K. Vaziri. 2007. Optimizing Scheduling of Post-Earthquake Electric Power Restoration Tasks. *Earthquake Engineering and Structural Dynamics*, **36**(2): 265-284.

Yan, S. and Y.L. Shih. 2009. Optimal scheduling of emergency roadway repair and subsequent relief distribution. *Computers and Operations Research*, **36**(6): 2049-2065.

Zhang, C., J.J. Kong, and S.P. Simonovic. 2018. Restoration resource allocation model for enhancing resilience of interdependent infrastructure systems. *Safety Science*, 102: 169-177.

Zolfaghari, M. R., and E. Peyghaleh. 2015. Implementation of equity in resource allocation for regional earthquake risk mitigation using two-stage stochastic programming. *Risk Analysis*, **35**(3): 434-458.